ОБЪЕДИНЕННЫЙ ИНСТИТУТ ЯДЕРНЫХ ИССЛЕДОВАНИЙ

E1 - 8061

K.Lanius

EXPERIMENTAL RESULTS ON EXCLUSIVE PROCESSES

Report given at the V International Symposium on Many Particle Hadrodynamics, June, 1974, Eisenach - Leipzig

Дубна 1974

E1 - 8061

K.Lanius

EXPERIMENTAL RESULTS ON EXCLUSIVE PROCESSES

Report given at the V International Symposium on Many Particle Hadrodynamics, June, 1974, Eisenach - Leipzig

1. Introduction

Up to now several hundred few-body production processes (multiplicity $n = 3$ and 4) with primary momenta up to ~ 30 GeV/c have been studied more or less incompletely. From these experiments, which may be considered as exploratory, much valuable information has been obtained.

During the last years few experiments with much better statistics have been done and experiments with usual statistics were combined to world data summary tapes respectively. Therefore a more complete use of the data could be made.

For my report on exclusive multi-particle production I selected a few experimental and methodical works which lead to a new quality in the study of production processes.

In the following two chapters some new results are described on few-body reactions and on new methods in order to analyse them.

The last chapter gives some results on many-body reactions ($n \geq 5$). The exclusive study of these collisions is until now at the beginning of exploration.

All the results which we get from the study of exclusive hadron production reactions with primary momenta up to ~ 70 GeV/c are also very important for understanding the same reactions at NAL or ISR energies. I think, that the gross features of these reactions are mainly the same for low primary momenta as well as for high primary momenta.

2. New Results on Partial Wave Analysis

After many years of studies of the A_1, A_3, Q and L enhancements a real progress was achieved with the help of the partial Wave Analysis, PWA, developed by the Illinois group [1]. This method allows investigation of the spin-parity structure of the produced three-meson systems and of the characteristic of their production mechanism.

The states produced were described in terms of $|J^P \ell M \eta\rangle$, where

J^P is the spin-parity of the three meson system,
M is the third component of J,
η is the naturality of the exchanged system, and
ℓ is the orbital angular momentum between the one meson and the two meson system.

2.1. Analysis of the (3π) system

The $(3\pi)^-$ system produced in the reaction $\pi^- p \to (\pi^-\pi^-\pi^+)p$ has been analysed by Ascoli et al. [1] from 5 to 25 GeV/c and by the CERN-Serpukhov Collaboration [2] at 25 and 40 GeV/c. The conclusion drawn from these analyses is that the A_1 and A_3 mass enhancements are not resonances, byt are produced by diffraction dissociation.

The $(3\pi)^+$ system produced in the reaction $\pi^+ p \to (\pi^+\pi^+\pi^-) p$ at 13 GeV/c has been analysed by Thompson et al. [3] and at 8, 16 and 23 GeV/c by the Aachen - Berlin - Bonn- CERN - Heidelberg Collaboration [4]. The results of these analyses are shown in fig. 1 and fig. 2 respectively. The general result is that these figures are strikingly similar to the figures for the $(3\pi)^-$ system.

In both experiments the $(3\pi)^+$ system is dominantly in unnatural spin-parity states 0^-, 1^+, 2^- and 3^+ and is produced in about 100% of the cases by natural parity exchange.

The density matrix element ρ_{00} in the Gottfried-Jackson system for $J^P = 1^+$ is in both experiments $\rho_{00} \sim 1.0$. This indicates t -channel helicity conservation. In the ABBCH-experiment it was found additionally, that $\mathrm{Re}\,\rho_{10} = -0.10 \pm 0.01$. This non-zero value of

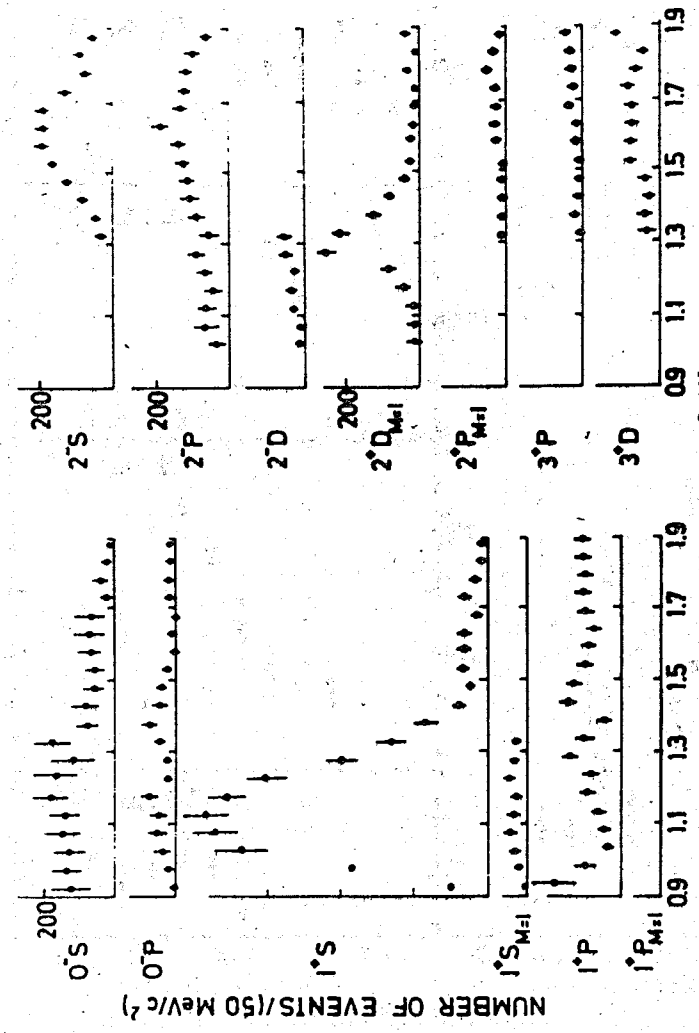

Fig. 1. Events of reaction $\pi^+ p \to \pi^+\pi^+\pi^- p$ in each $|J^P \ell M\rangle$ state as a function of $M(3\pi)^+$ in bins of 50 MeV with $|t'| \leq 0.5\ (\mathrm{GeV/c})^2$.

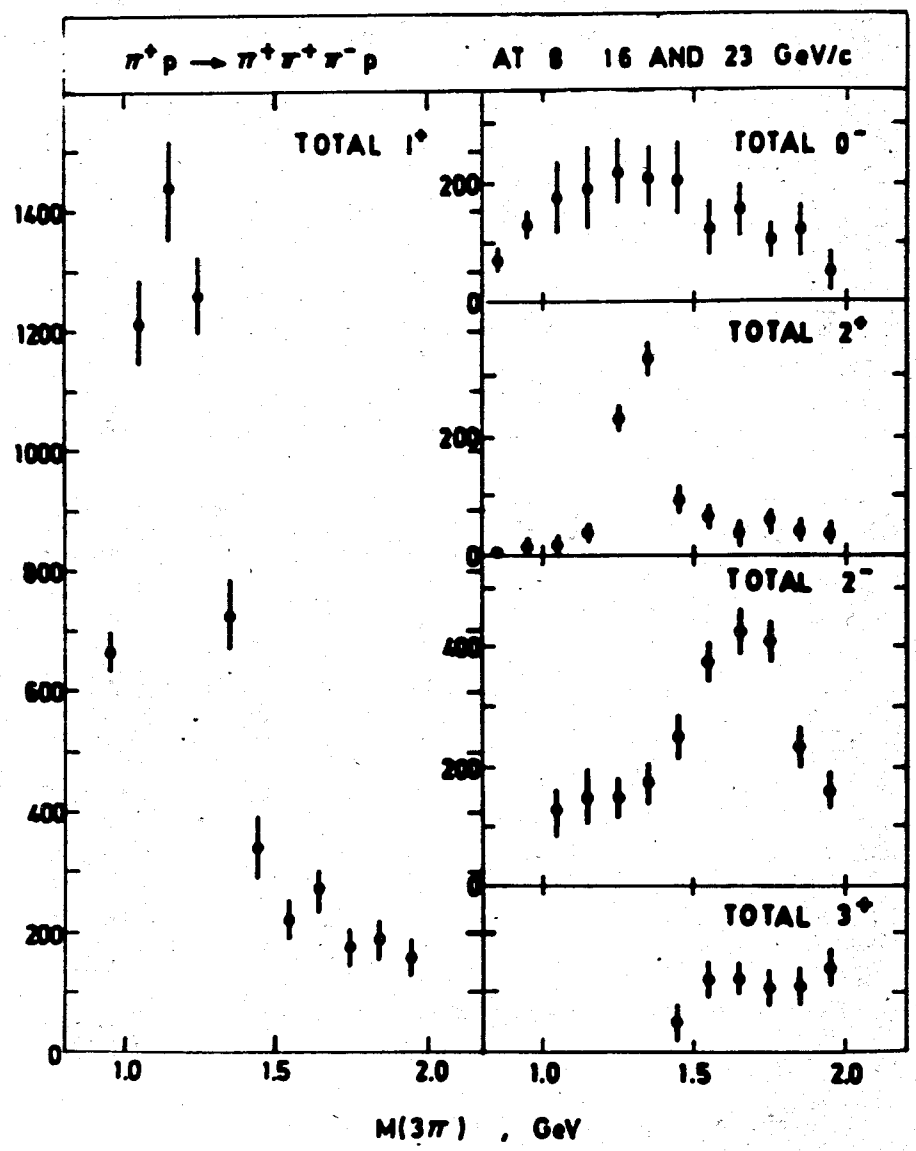

Fig. 2 a). Events of reaction $\pi^+ p \rightarrow \pi^+\pi^+\pi^- p$ in each J^P state as a function of $M(3\pi)^+$ in bins of 100 MeV with $|t'| < 0.8$ $(GeV/c)^2$.

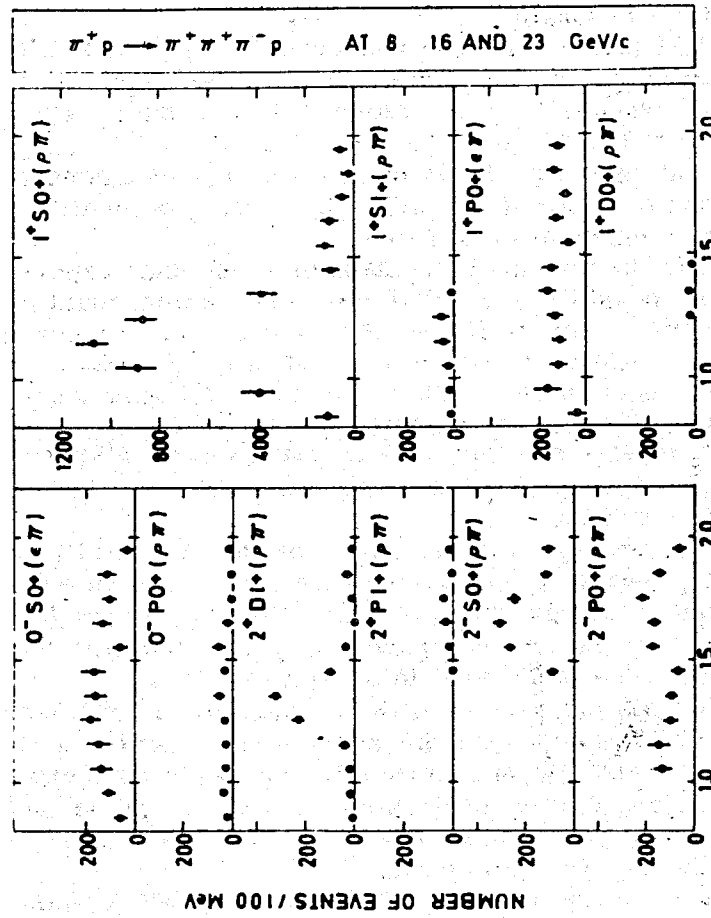

Fig. 2b). Dependence of $|J^P \ell\, M\eta>$ states on the $(3\pi)^+$ mass.

$Re\rho_{10}$, which is more sensitive to small admixtures of helicity ± 1, indicates however, that helicity conservation is only approximate.

In fig. 3 the phase differences $\Psi(J^P\ell)=$ (phase 2^-S) - (phase $J^P\ell$) are plotted for all other included $J^P\ell$ as a function of mass [3]. The results show a variation consistent with a resonant A_3 .

A similar phase variation was reported by the ABBCH-Collaboration. In the A_3 mass region the phase difference $\Psi =$ [phase $2^-S(f\pi)$] - [phase $0^-S(\epsilon\pi)$] shows a variation of about 100° through the full width of 2^-S mass enhancement (see fig. 4). Both results are not inconsistent with the data of ref. [1] at 11 - 25 GeV/c, however the phase seems constant at 40 GeV/c [2].

In order to interpret the data of these four experiments one possibility is that the A_3 region could be more complex, with both a resonant and a non-resonant component present. The constancy of the 2^-S phase at 40 GeV/c may indicate that the resonant component disappears with increasing energy.

In both experiments the weak variations of the 1^+S phase in the A_1 region suggest that A_1 cannot be considered as a single resonance.

Ascoli et al. [5] use the phase of the A_1^- amplitude from a Reggeized Deck model calculation and the A_2^- phase from a Regge fit to $d\sigma/dt$ for A_2, to predict the $A_2^- - A_1^-$ phase and compare the prediction with the phase difference observed in $\pi^-p \to \pi^+\pi^-\pi^-p$ (see fig. 5). For all momentum transfer bins and all incident momenta (5 - 40 GeV/c) the agreement is within 30° (solid line). This depends crucially on the contribution of the Reggeized pion propagator to the A_1 phase and requires equal signs for the f° and the Pomeron residues in the A_2 amplitude.

The 2^+D state in the A_2 region shows a phase variation consistent with resonance behaviour.

In both experiments the differential cross section of all the states shows a peak at small t' except for 2^+D which has a pronounced dip in the forward direction (see fig. 6).

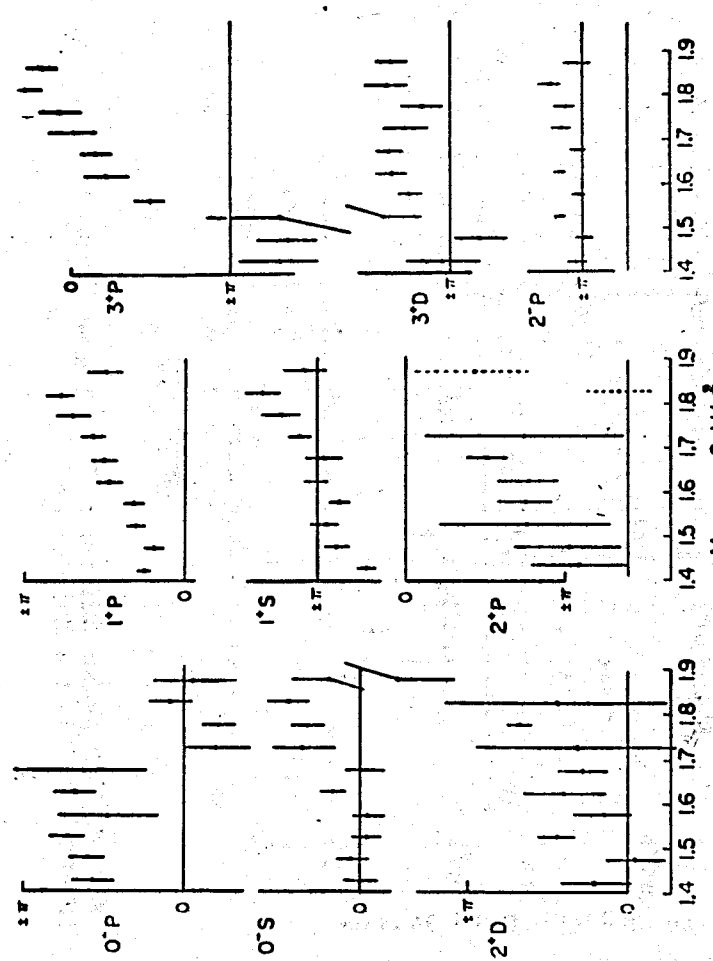

Fig. 3: The phase difference $\Psi(J^P\ell)=$(phase 2^-S) - (phase $J^P\ell$) for all other contributing states as a function of $M(3\pi)^+$.

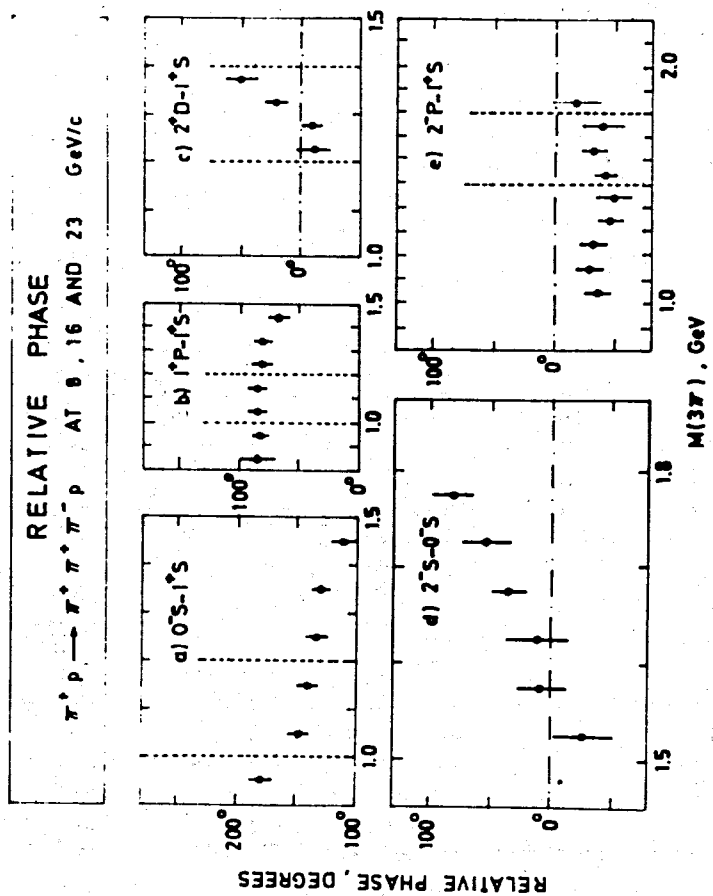

Fig. 4. The phase difference $\Psi = [$ phase $2^-S(f\pi)] - [$phase $0^-S(\epsilon\pi)]$ as a function of $M(3\pi)^+$.

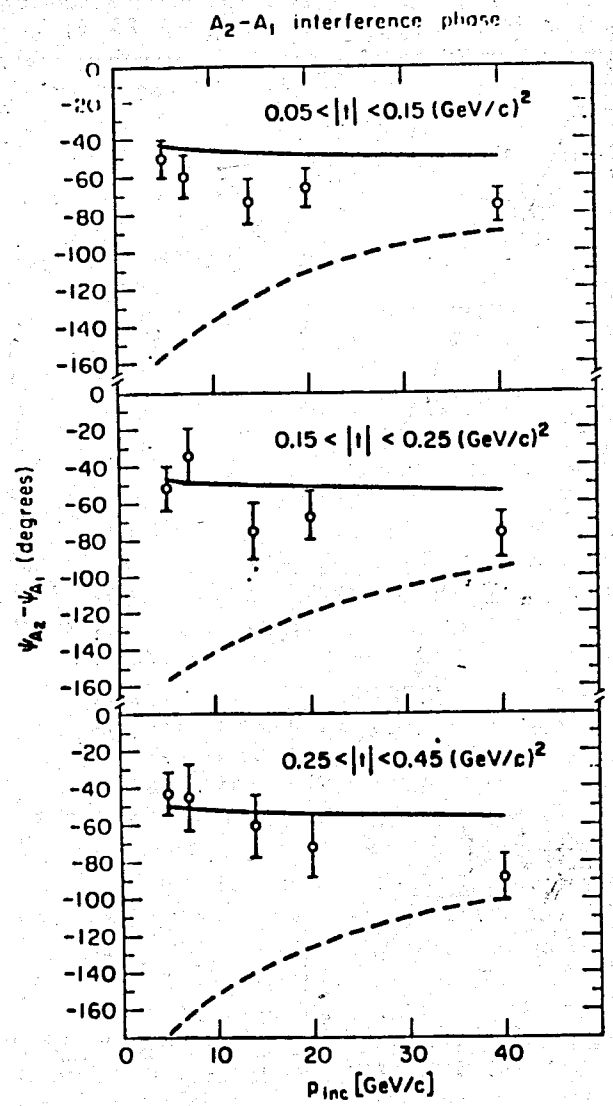

Fig. 5. Comparison of measured $A_2 - A_1$ interference phase to the phase predicted from Regge and Deck model calculation (solid curve).

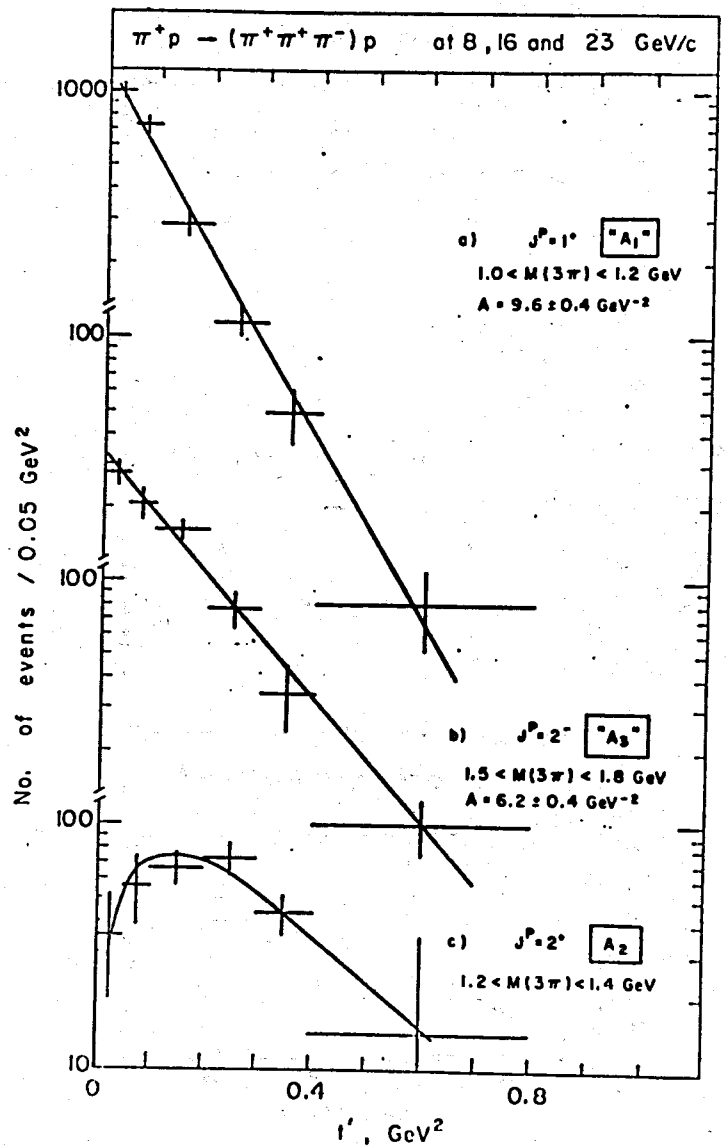

Fig. 6. t' dependence of $J^P = 1^+, 2^-$ and 2^+ states. The quantity A is the slope of the exponential fits.

2.2. Analysis of the $(K\pi\pi)$ system

The $(K^-\pi^+\pi^-)$ system produced in the non charge exchange reaction $K^-p \rightarrow (K^-\pi^+\pi^-)p$ at 10 and 16 GeV/c has been analysed by the Aachen - Berlin - CERN - London - Vienna Collaboration [6], at 14.3 GeV/c by the Rutherford -Ecole Polytechnique - Saclay Collaboration [7] and at 40 GeV/c by the CERN - Serpukhov Collaboration [8].

The main $|J^P M\eta>$ states are shown in fig. 7. It has been found that:

(i) $M = 0$ is dominant, which means that t -channel helicity conservation approximately holds.

(ii) The $(K\pi\pi)^-$ system is dominantly produced in unnatural J^P states 0^-, 1^+, 2^-, 3^+, with contributions from six decay modes $K^*(890)\pi$, $K^*(1420)\pi$, $K\rho$, Kf°, $K\pi$ and $K\epsilon$ (see fig.8).

(iii) The $(K\pi\pi)$ system is produced dominantly by natural parity exchange (fig. 8).

(iv) The weak variation of the 1^+S phase in the Q -region suggests that the Q enhancement cannot be considered as a single resonance (fig. 9).

(v) More than one decay mode and J^P state are required to describe the Q and L enhancements (see fig. 10), which must therefore be considered as complex structures due to the summation of several partial waves.

(vi) Overall, the production mechanism of the $(K\pi\pi)^-$ system is similar to that of the $(3\pi)^\pm$ system.

A Partial Wave Analysis of the $(K\pi\pi)^\circ$ system produced in the charge exchange reaction $K^-p \rightarrow (K^\circ\pi^+\pi^-)n$ has been made in the mass range $1{,}04 < M(K\pi\pi)^\circ < 1.56$ GeV combining data at 8, 10 and 16 GeV/c [9]. The K° decay was visible and measurable. The analysis was made in the mass interval 1.04 - 1.56 GeV, which is the region of greatest interest for comparison with the Q -region of the corresponding $(K\pi\pi)^-$ system.

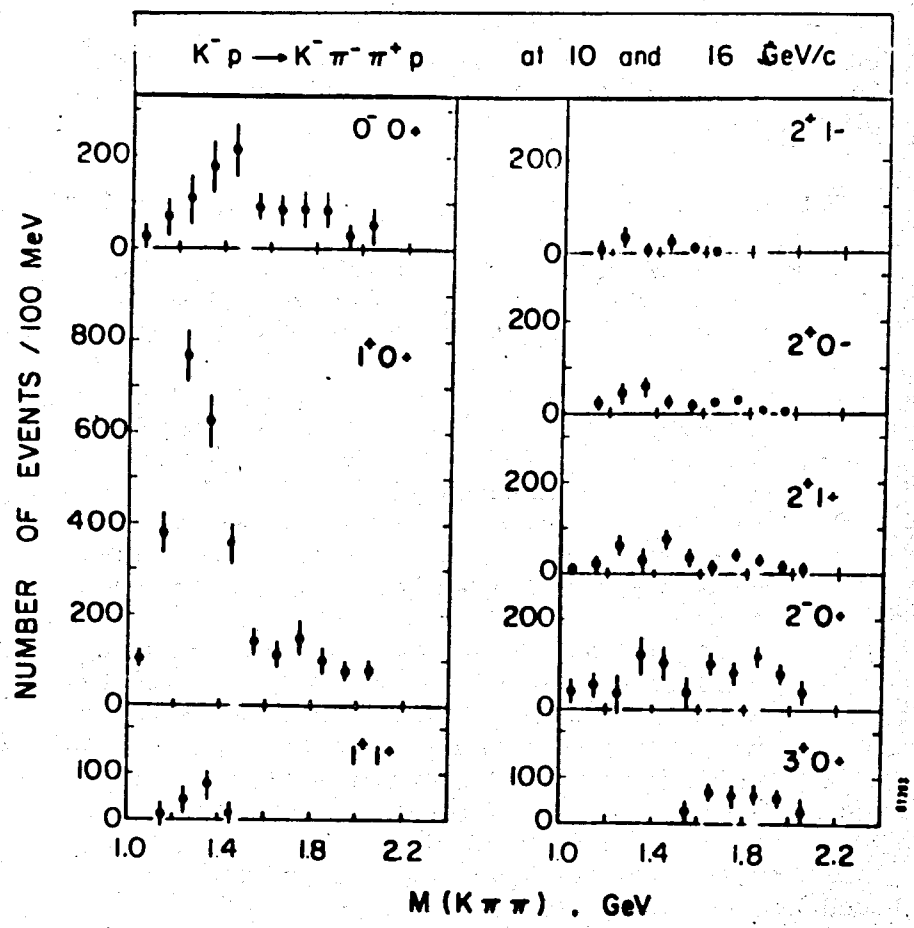

Fig. 7 a). Number of events in each $|J^P M\eta>$ state, as a function of $M(K\pi\pi)^-$ in bins of 100 MeV with $|t'|<$ < 0.8 (GeV/c)^2.

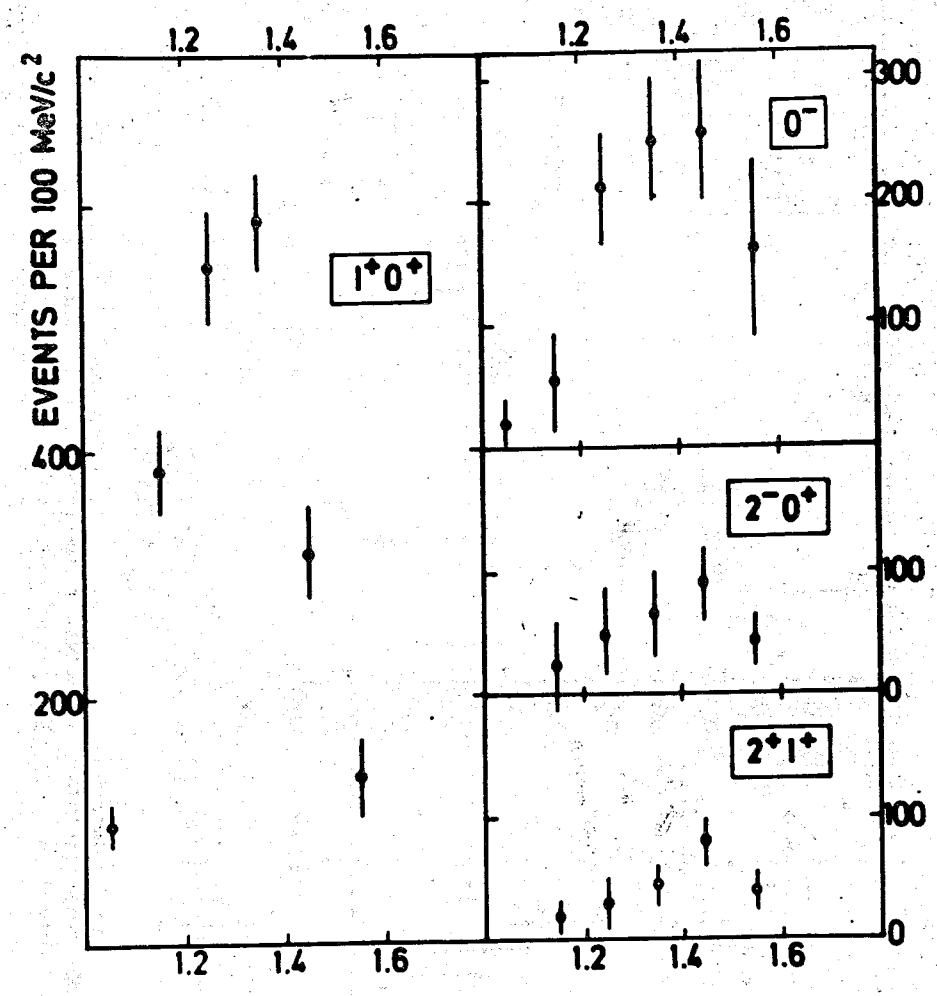

Fig. 7b). Number of events in the 4 dominant $|J^P M\eta>$ states as a function of $M(K\pi\pi)^-$ in bins of 100 MeV with $|t'| < 0.8$ (GeV/c)^2.

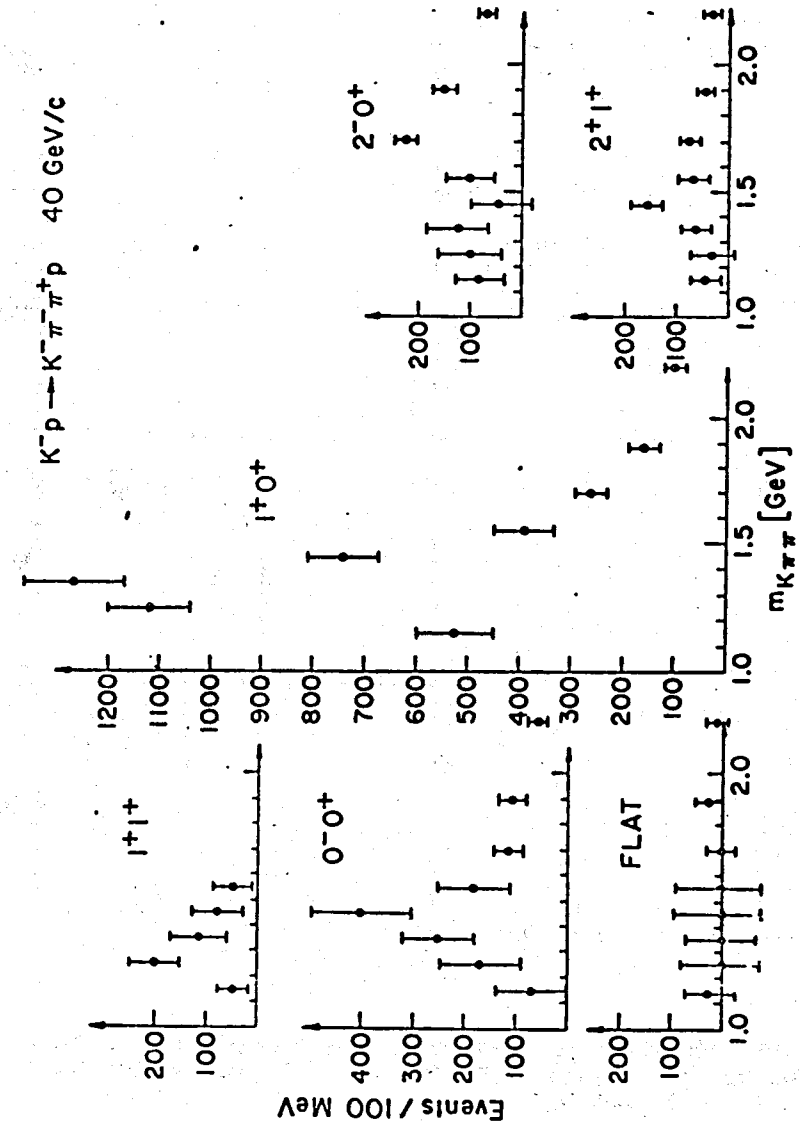

Fig. 7c). Number of events in each $|J^P M\eta>$ state, as a function of $M(K\pi\pi)^-$ in bins of 100 MeV.

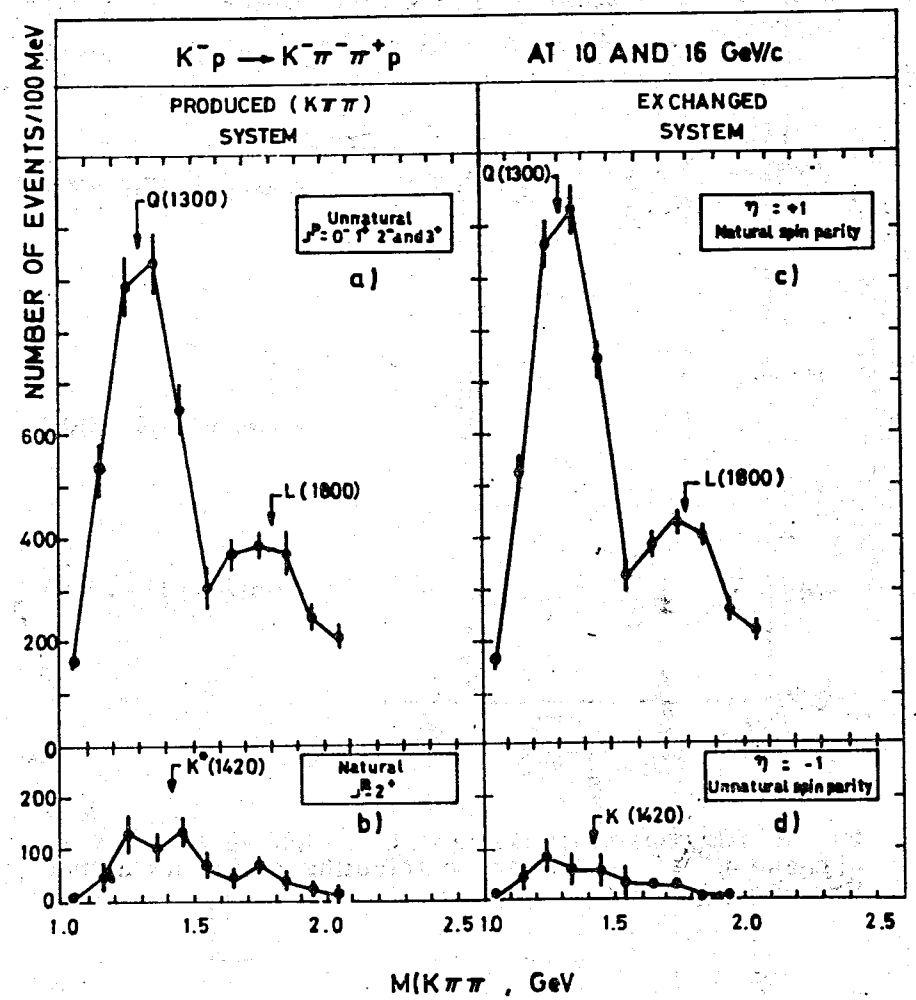

Fig. 8 a) and b): Comparison of the number of events having the $(K\pi\pi)^-$ system in states of unnatural and of natural spin-parity. c) and d): Comparison of the number of events for which the reaction $K^-p \to (K^-\pi^-\pi^+)p$ proceeds via the exchange of natural and of unnatural spin-parity.

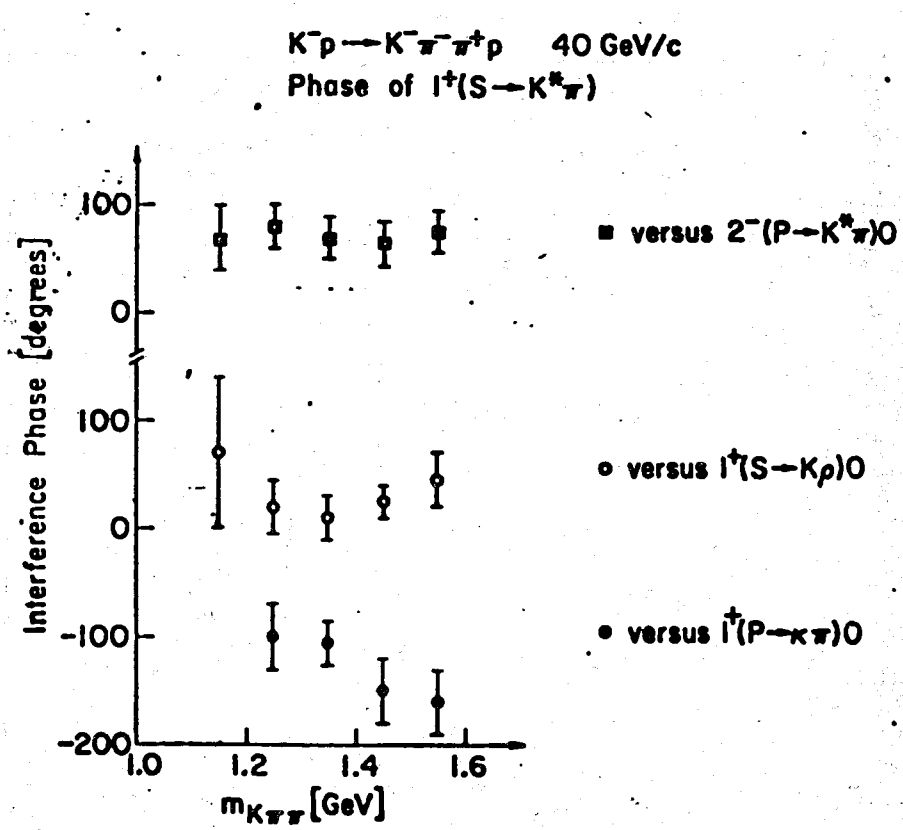

Fig. 9. The phase difference $\Psi(J^P \ell) = [\text{phase } 1^+S(K^*\pi)] - [\text{phase } J^P \ell]$ for other contributing states as a function of $M(K\pi\pi)$.

It was found that:

(i) In about 2/3 of the events, the $(K\pi\pi)^\circ$ system is produced in unnatural spin-parity states 0^- (24% and 1^+ (43%).

(ii) The unnatural spin-parity states are produced mostly (~ 80%) of the events) by natural parity exchange.

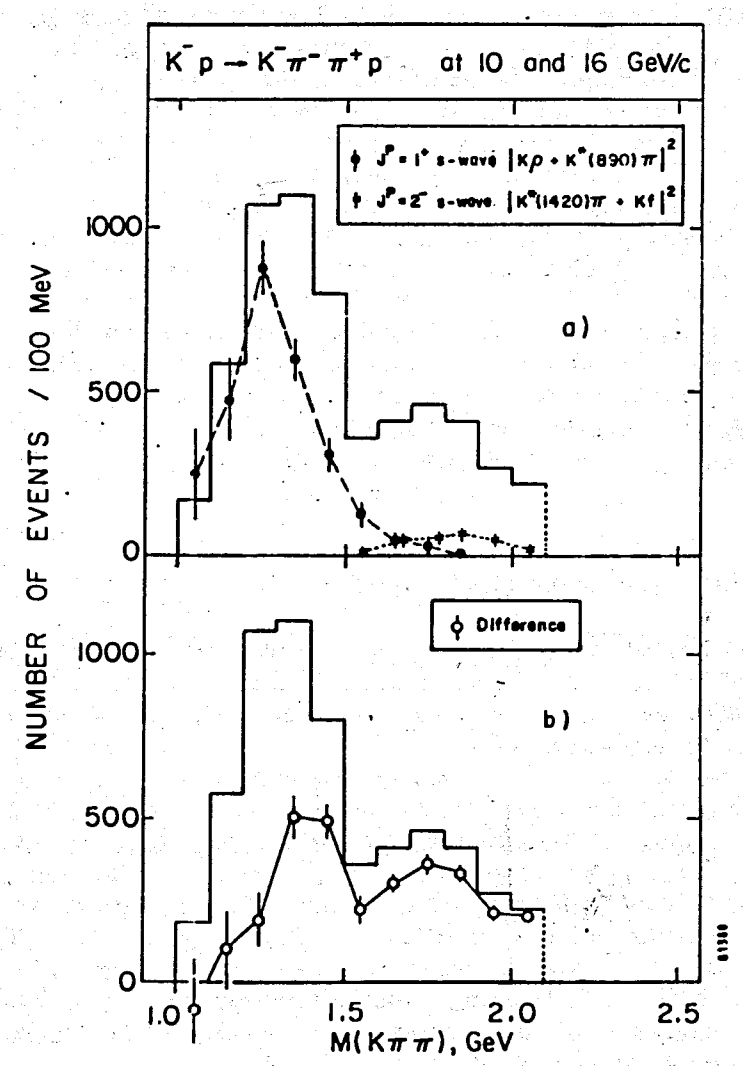

Fig. 10. a) Comparison of the experimental mass spectrum with the contributions of i) the $K\rho$, $K^*(890)\pi$ and $K\rho/K^*(890)\pi$ interference from the state $J^P = 1^+S$ –wave (solid circles) and ii) the $K^*(1420)\pi$, Kf and $K^*(1420)\pi/Kf^\circ$ interference from the state $J^P = 2^-S$– wave (crosses). b) Difference (open circles) between the total mass spectrum and the sum of the two contributions from $J^P = 1^+$ and $J^P = 2^-$.

(iii) About 1/3 is produced in the natural spin-parity state $J^P = 2^+$. This number is compatible with the number calculated using the 2^+ part of the cross section from the reaction $K^- p \to (K^- \pi^+) n$ and the $K\pi / K\pi\pi$ branching ratio. Hence, the 2^+ state is consistent with being all $K^*(1420)$.

These facts, that unnatural J^P states are produced in this non-diffractive channel, that $J^P = 1^+$ is dominant and that the exchange responsible for their production is mostly of natural parity, are similar to what was found for the charged $(K\pi\pi)^-$ system in the diffractive reaction $K^- p \to (K\pi\pi)^- p$. This implies, that the presence of unnatural spin-parity states produced by natural parity exchanges cannot be considered as an exclusive characteristic of diffractive processes.

2.3. Analysis of the $(K\pi)$ system

A partial wave analysis has been performed for the $(K^-\pi^+)$ system produced in the reaction $K^- p \to K^- \pi^+ n$ at 10 and 16 GeV/c by the Aachen - Berlin - CERN - London - Vienna Collaboration /10/.

Though the $(K^-\pi^+)$ mass spectrum is rather well understood there are still open questions, e.g., whether an isospin 1/2 S -wave resonance is present. Evidence for a broad S -wave $(K\pi)$ enhancement centered at ~ 1300 MeV, which could be interpreted as a resonance, has recently been reported by Cords et al. /11/. The results from phase shift analyses performed on the $(K\pi)$ system are either ambiguous or give contradictory values for the mass and width of the claimed S -wave resonance /12/.

Fig. 11 shows the results of the analysis:

(i) Production of the $K^*(980)$ in helicity zero state by unnatural parity exchange and in helicity ± 1 by natural parity exchange.

(ii) Production of the $K^*(1420)$ again in both helicity states.

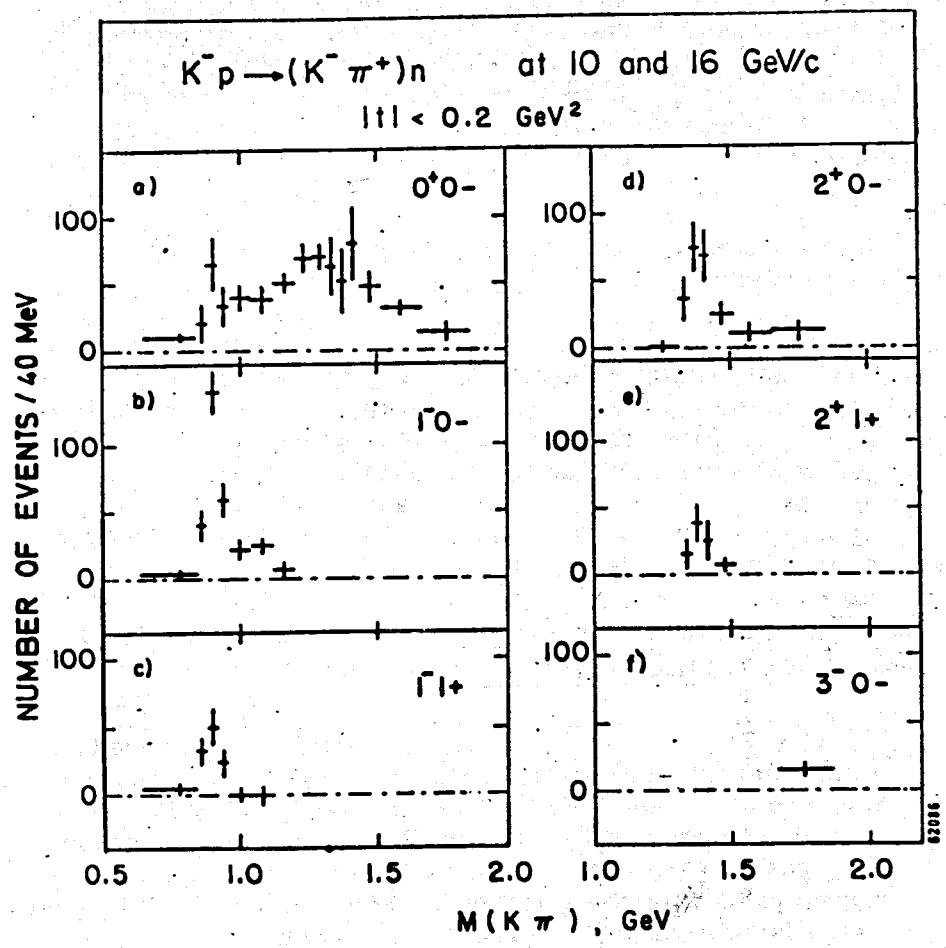

Fig. 11. Number of events in each $|J^P M\eta>$ state as a function of $M(K^-\pi^+)$.

(iii) The S -wave $(K^-\pi^+)$ system is consistent with a Breit-Wigner shape peaked at 1.25 GeV and 0.5 GeV wide.

(iv) The $(K^-\pi^+)$ S -wave has the biggest cross section of all the states present in the sample

($70 \pm 4\,\mu b$ at 10 GeV/c and $19 \pm 2\,\mu b$ at 16 GeV/c). This energy dependence is consistent with an $s^{2\alpha-2}$ behaviour where $\alpha = t$, as expected for pure π-exchange.

3. Multidimensional Analysis of Few-Body Hadron Collisions

In the field of few-body collisions some new results have been gained in the last one or two years. This is due to new results by application of the Prism Plot Analysis, PPA, introduced by Pless et al.[13] but also by introducing modifications of the PPA.

The most important modification of the multidimensional analysis is the Analytical Multi-Channel Analysis proposed by Van Hove[14].

3.1. New results of the PPA

The Prism Plot Analysis is an iterative procedure which separates reaction channels which contribute to the same n-body final state by assigning each event to a chosen channel hypothesis. This is done by comparing the position of each event in the $3n-5$ dimensional hyperspace with the position of Monte Carlo events generated for the different channel hypotheses.

To generate events the PPA neglect possible interference effects. The method uses therefore $3n-5$ one dimensional distributions $D_i^j(x_i)$ $(i=1\ldots 3n-5)$ for each hypothesis j. The $D_i^j(x_i)$ are the effective mass distributions and the production and decay angular distributions.

The real events are tagged according to the number of Monte Carlo events of each channel hypothesis in its neighbourhood. A simple way to specify the neighbourhood is to define a $3n-5$ dimensional hypercube.

The PPA will give the best results for small boxsizes in order to reduce the overlap between different channels, and for large numbers of generated Monte Carlo events.

Bastien et al.[15] have applied the PPA to a sample of about 3100 events of the reaction $\bar{p}p \to \bar{p}p\,\pi^+\pi^-$ at 5.1 GeV/c. The aim was to search for the channels

$$\bar{p}p \to (p\,\pi^+\pi^-)_{DD}\,\bar{p}$$

$$\bar{p}p \to (\bar{p}\,\pi^+\pi^-)_{DD}\,p\ .$$

As is well known the quasi two-body channel $pp \to \Delta^{++}\bar{\Delta}^{--}$ has been found to dominate the reaction. In order to look for the less prominent three particle dissociations the $(p\pi^+)-$ and $(\bar{p}\pi^-)$-system respectively have been combined into a single pseudo-particle and treated the sample as a three particle final state with PPA.

Figures 12 and 13 show the two and three body mass distributions for the selected events. In conclusion, a sizeable diffractive component is present which accounts for ~ 30% of the final state at this energy. The data for the dissociation of the proton, or antiproton, have invariant mass spectra, dynamical properties, and cross sections similar to what is found with pion and proton beams.

Ferrando et al.[16] have applied the PPA to a sample of 19 442 $\pi^-p \to \pi^+\pi^-\pi^-p$ events at 3.9 GeV/c. They introduce the following channels:

(1) $\pi^-p \to pA_1^-$, $A_1^- \to \rho^\circ\pi^-$, $\rho^\circ \to \pi^+\pi^-$

(2) $\pi^-p \to pA_2^-$, $A_2^- \to \rho^\circ\pi^-$, $\rho^\circ \to \pi^+\pi^-$

(3) $\pi^-p \to N^{*\circ}(1520)\rho^\circ$, $N^{*\circ}(1520) \to p\pi^-$, $\rho^\circ \to \pi^+\pi^-$

(4) $\pi^-p \to N^{*\circ}(1688)\rho^\circ$, $N^{*\circ}(1688) \to p\pi^-$, $\rho^\circ \to \pi^+\pi^-$

(5) $\pi^-p \to \Delta^\circ(1236)\rho^\circ$, $\Delta^\circ(1236) \to p\pi^-$, $\rho^\circ \to \pi^+\pi^-$

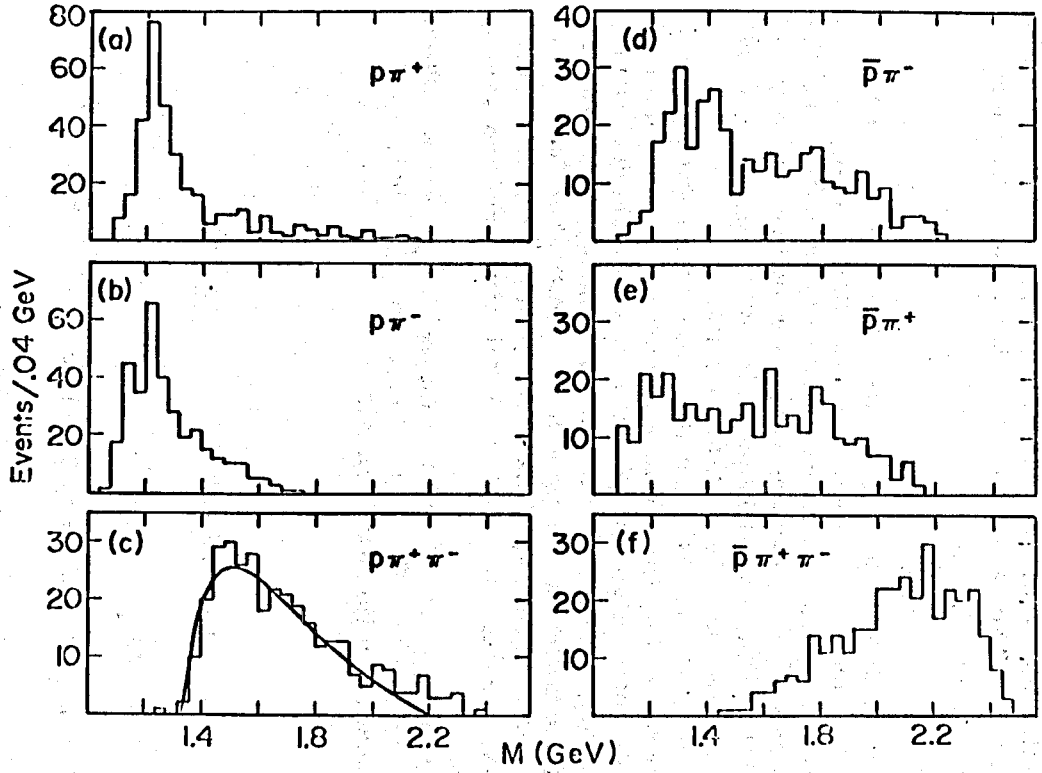

Fig. 12. Two and three body invariant mass plots for events identified as diffraction of the proton. The curve on Fig. 12c represents the diffractive shape found in π^+ p interactions.

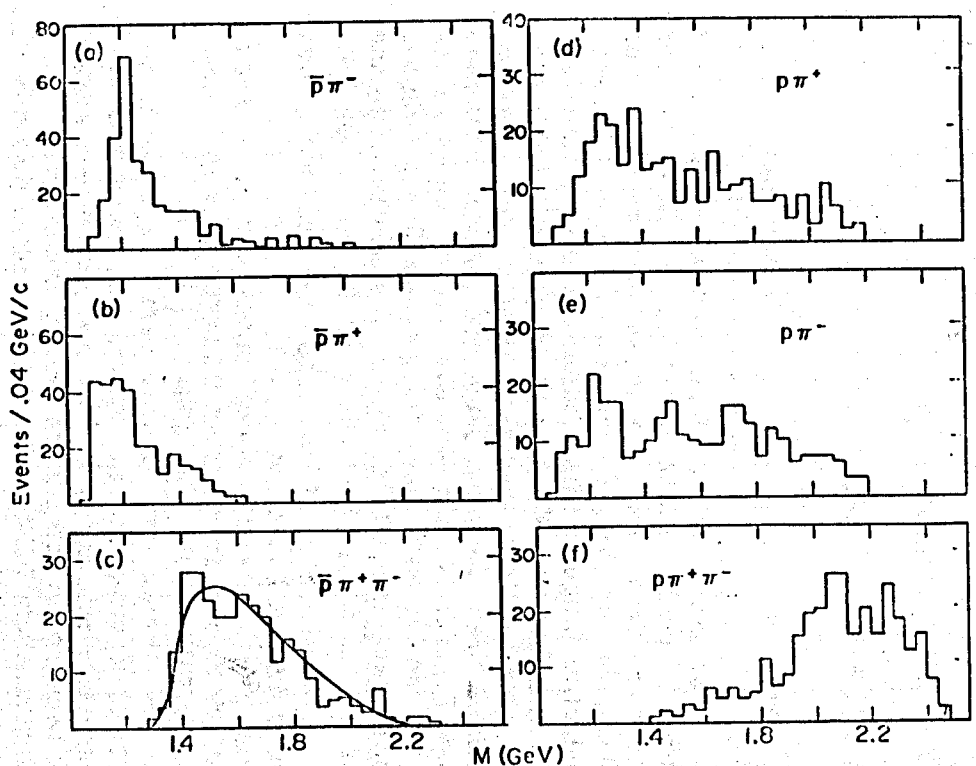

Fig. 13. Two and three body invariant mass plots for events identified as diffraction of the antiproton. The curve is the same as on fig. 12c.

(6) $\pi^- p \to \Delta^{++}(1236)\pi^-\pi^-$, $\Delta^{++}(1236) \to p\pi^+$

(7) $\pi^- p \to (DD)\pi^-$, $(DD) \to \Delta^{++}\pi^-$, $\Delta^{++} \to p\pi^+$

(8) $\pi^- p \to (DD)\pi^-$, $(DD) \to p\pi^+\pi^-$

(9) $\pi^- p \to p\pi^- f^\circ$, $f^\circ \to \pi^+\pi^-$

(10) $\pi^- p \to p\pi^+\pi^-\pi^-$ (phase space).

For the first step, Monte Carlo events are generated according to phase space modified by Breit-Wigner functions and diffraction like mass distributions. For the subsequent iterations, the authors also introduce the production angular distributions and the Gottfried-Jackson and Treiman-Yang decay angles of each resonance as obtained from the previous step. Some physical distributions after the separation are given as examples in fig. 14. Figures 14a and 14b show the 3π mass distributions for the channels pA_1 and pA_2. Masses and shapes agree with expected values. The ρ signal induced by the decay of A_2 in the pA_2 channel can be seen in fig. 14c.

The contamination of the different channels was checked by different methods:

- Through mass spectra which should not show resonance production from other channels after the selection operated by PPA (see table 1).
- In the A -region through spin parity analysis of the $(\pi^+\pi^-\pi^-)$-system. It was shown, that more than 40% of the events labelled pA_1 or pA_2 must be classified as background coming from other channels.
- Through a study of the PPA with simulated events. It shows that the large overlap observed between the channels have a physical origin.

The authors came to the conclusion that at this relatively low energy and at such a complex final state large overlap regions between channels are present.

Table 1

RATES AND CONTAMINATIONS AFTER 13 ITERATIONS

? Not able to estimate

0 No apparent contamination

	Rates (%)	Number of events	Contaminated channels (in nb. of events). The origin of the contamination is indicated in the first column										Total losses (lower limit)
			pA_1	pA_2	$N^\circ_{1520}\rho^\circ$	$N^\circ_{1688}\rho^\circ$	$\Delta^\circ\rho^\circ$	$\Delta^{++}\pi^-$	$DD(\Delta^{++}\pi^-)\pi^-$	$DD(p\pi^+\pi^-)\pi^-$	$p\pi^-f^\circ$	ph. sp.	
pA_1	13.1	2538			0	15	20	0	0	0	0	0	35
pA_2	11.7	2267			15	0	20	40	68	0	0	18	161
$N^\circ_{1520}\rho$	8.5	1654	75	46		20	0	20	0	0	0	0	161
$N^\circ_{1688}\rho$	10.7	2077	100	25	0		0	40	0	0	0	0	165
$\Delta^\circ\rho$	11.9	2313	50	70	0	66		50	?	0	0	0	236
$\Delta^{++}\pi^-$	9.2	1793	250	46	104	130	130		?	?	42	30	902
$DD(\Delta^{++}\pi^-)\pi^-$	17.5	3409						?					?
$DD(p\pi^+\pi^-)\pi^-$	10.5	2050											?
$p\pi^-f^\circ$	3.7	728	?	?	20	20	46	0	0	0		0	86
ph. sp.	3.1	614											
Total contamination (lower limit)			475	187	139	251	386	150	68	0	42	46	

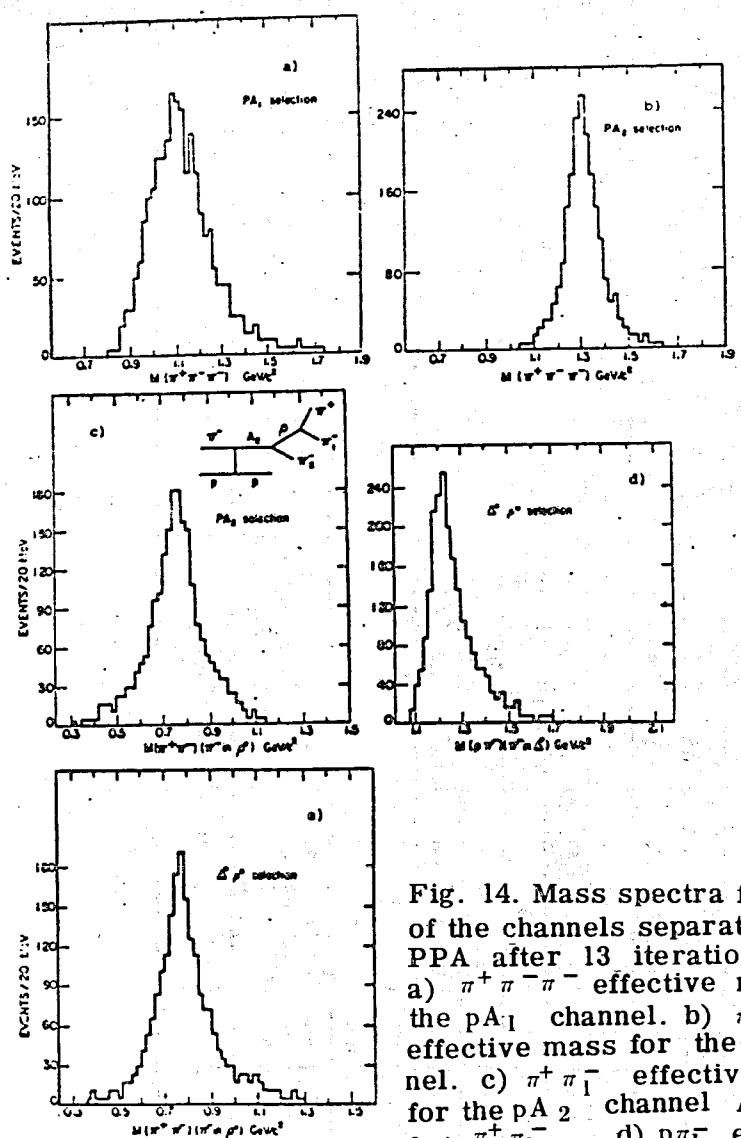

Fig. 14. Mass spectra for some of the channels separated by the PPA after 13 iterations: a) $\pi^+\pi^-\pi^-$ effective mass for the pA_1 channel. b) $\pi^+\pi^-\pi^-$ effective mass for the pA_2 channel. c) $\pi^+\pi_1^-$ effective mass for the pA_2 channel $A_2 \to \rho\pi_2^-$; $\rho \to \pi^+\pi_1^-$. d) $p\pi_1^-$ effective mass for the $\Delta^{\circ}\rho^{\circ}$ channel $\Delta^{\circ} \to p\pi_1^-$, $\rho^{\circ} \to \pi^+\pi_2^-$, e) $\pi^+\pi_2^-$ effective mass for the $\Delta^{\circ}\rho^{\circ}$ channel $\Delta^{\circ} \to p\pi_1^-$, $\rho^{\circ} \to \pi^+\pi_2^-$.

In order to get better results there are the following possibilities:

- to go to lower multiplicity,
- to go to higher energy,
- to develop new methods to deal with the complexities due to the overlaps and interference effects.

P.J.Dornan and B.Pollock [17] proposed a new variant of the PPA method. In order to reduce the necessary computing time of the Monte Carlo generation Dornan and Pollock assume that the distribution of events $D_i^j(x_i)$ for each hypothesis j can be written for a 3 particle final state:

$$D_i^j(x_1,x_2,x_3,x_4) \doteq D_1^j(x_1)D_2^j(x_2)D_3^j(x_3)D_4^j(x_4).$$

From these one-dimensional distributions the probability that a real event is one of the type j is defined

$$P_j = f_1^j f_2^j f_3^j f_4^j F^j .$$

Where f_i^j is the fraction of events in D_i^j in the same bin as the real event. F^j is the overall fraction of events in channel j.

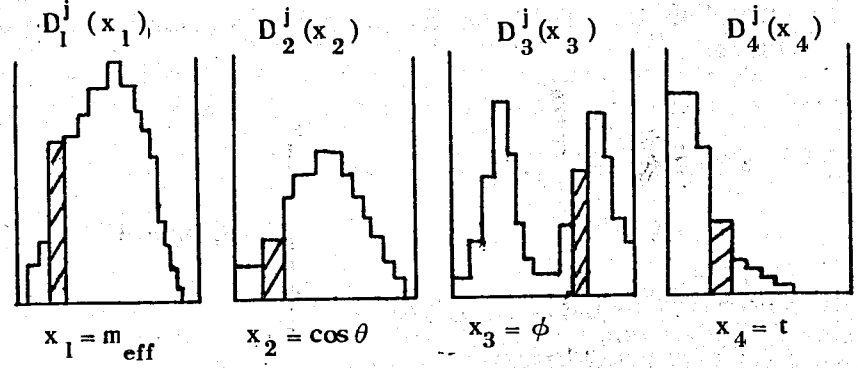

To take background into account in addition P_j (BKG) was calculated

$$P_j(BKG) = g_1^j g_2^j g_3^j g_4^j G^j ,$$

where the g_i^j are calculated from background distributions. One event is tagged as belonging to hypothesis j if $P_j > P_j$ (BKG) or to background if P_j (BKG)$> P_j$ and if there is no other channel j′ such that $P_j > 10 P_{j'}$. If one event is tagged by more than one hypothesis it is weighted according to the probabilities. The tagged events are used to replot the distributions for use in the next iteration. Background is taken into account after the first iteration with all distributions flat.

3.2. Analytical multi-channel analysis

An important modification of the PPA was recommended by Van Hove /14/. He proposed the use of analytically defined amplitudes whenever overlap between channels occurs. In this way it is possible to treat interference between channels.

The reaction $K^+p \to K^\circ\pi^+p$ has been analysed using analytical amplitudes in the multidimensional space. Very preliminary results at 5 GeV/c /18/ and at 12 GeV/c * /19/ were presented at the Topical Conference on Multidimensional Analysis of Hadron Collisions at CERN. In this reaction the following channels are considered

$K^+p \to K^{*+}(890)p$
$\to K^{*+}(1420)p$
$\to (K\pi)_{\text{backgr.(s-wave)}}p$
} Channel I

$\to K^\circ\Delta^{++}(1236)$ Channel II

Other weak channels are neglected.

---

* Data from World K^+ Collaboration.

The first step of the method is to start with some guess amplitudes A for the two channels considered. A simple choice could be

$$A(t, m^2, \theta, \phi) = \sum R(t) \cdot B(m) \cdot d(\theta, \phi)$$

Production B.W. Decay correlation **

For the two amplitudes A_I and A_{II} the following definitions are used:

$$f_1 = |A_I|^2 \,, \; f_2 = |A_{II}|^2 \,, \; f_3 = 2\,\mathrm{Re}\, A_I^* A_{II}$$

$$|A|^2 = |A_I + A_{II}|^2 = f_1 + f_2 + f_3 \,.$$

From these f -values the samples are selected in the following way. For each event

- compute $R_i = \dfrac{f_i}{f_{i\,(\max)}}$ $(i = 1,2)$
- select a cut-off $\epsilon \sim 1 - 5\,\%$
- if $R_1 > \epsilon$ and $R_2 < \epsilon$, i.e., dominating channel I;
  if $R_2 > \epsilon$ and $R_1 < \epsilon$, i.e., dominating channel II;
  if $R_1 > \epsilon$ and $R_2 > \epsilon$, i.e., overlap I - II.

The interference sample is a part of overlap sample I - II. For these selected samples each event is weighted

$$w_1 = \frac{f_1}{f_1 + f_2 + f_3} \,; \; w_2 = \frac{f_2}{f_1 + f_2 + f_3} \,; \; w_3 = \frac{f_3}{f_1 + f_2 + f_3}$$

$$w_1 + w_2 + w_3 = 1$$

If $A = A_I + A_{II}$ is correct, the weighted distribution of events in sample I is described by amplitude A_I, and in sample II by amplitude A_{II} and sample I-II corresponds to distribution of interference term in phase space.

** At 5 GeV/c the density matrix elements are taken from a modified version of the Illinois Partial Wave Analysis programm /10/.

Hence the weighted distribution can be used to improve the choice of amplitudes. The second step of the method is the same as the first, but using new $A_I A_{II} \ldots$.

At 5 GeV/c a sample of 1719 events was analysed. After the first step of the method with a cut-off $\epsilon = 2\%$ the preliminary results look promising. Figure 15 shows as one example a comparison of three different separation methods on the K*(1420) sample. You see that the analytical method gives a better separation.

At 12 GeV/c the same sample was analysed with the analytical method which before was analysed with the PPA method [20]. Figure 16 shows the mass distribution of $K^\circ\pi^+$ for sample I, overlap and interference. You see that overlap and therefore interference at 12 GeV/c are small.

Figure 17 shows the mass distribution of $p\pi^+$ for sample II, overlap and interference. The overlap events lie in the $\Delta^{++}(1236)$ region.

Most of the decay angular distributions look as expected (see for example fig. 18). However by changing the cut-off value from 2% to $\epsilon = 5\%$ the distributions look more symmetric and peaked (fig. 19).

The properties of the remaining events with R_I and $R_2 < \epsilon$ can be seen in fig. 20. There are indications of structure in $K^\circ\pi^+$ mass at ~1760 MeV and in $p\pi^+$ mass at ~1890 MeV.

The present results are encouraging enough to go on with the new method of analysis.

4. Analysis of Many-Body Hadron Collisions

While one can say for good reasons that the study of the few-body reactions has reached a qualitatively new level, our knowledge of the exclusive many-body reactions ($n \gtrsim 5$) are still fragmentary. In the following a few new experimental results with known methods and a new method for the study of many-body reactions shall be described.

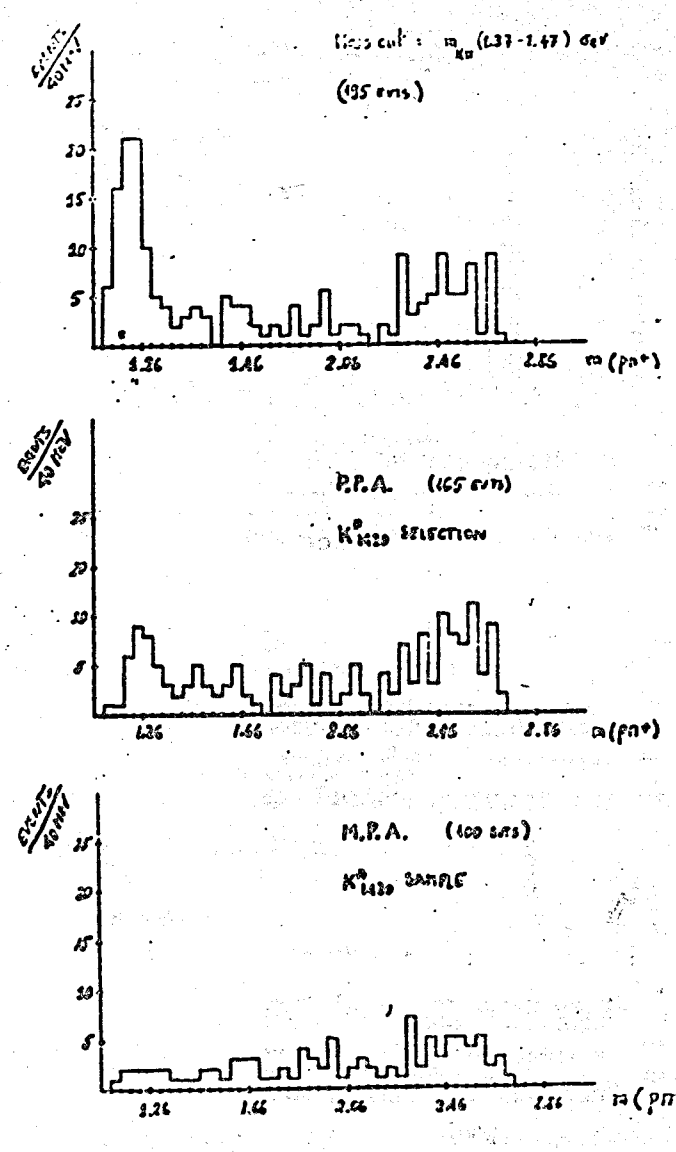

Fig. 15. Comparison of three different separation methods on the K*(1420) sample.

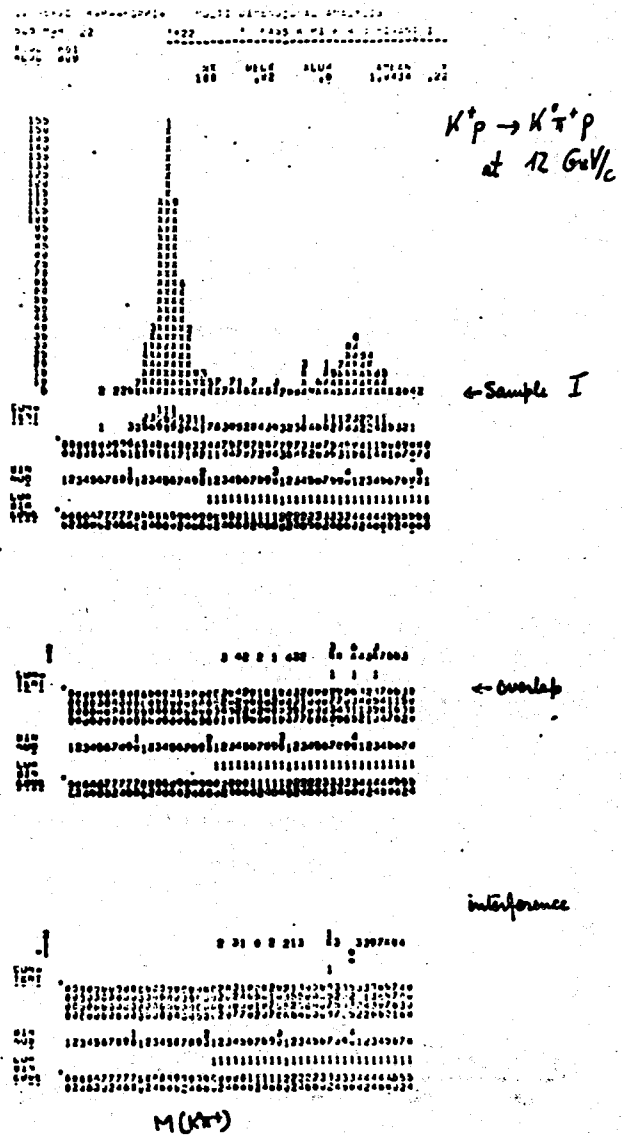

Fig. 16. Mass distribution $M(K^0\pi^+)$ for sample I, Overlap and interference distribution.

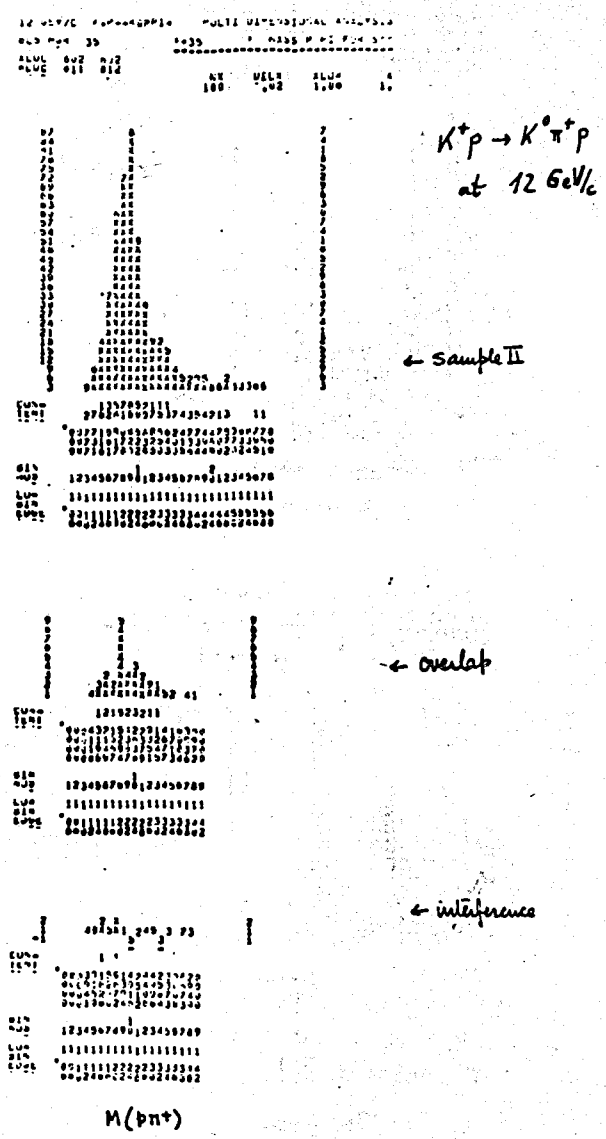

Fig. 17. Mass distribution $M(p\pi^+)$ for sample II, overlap- and interference-distribution.

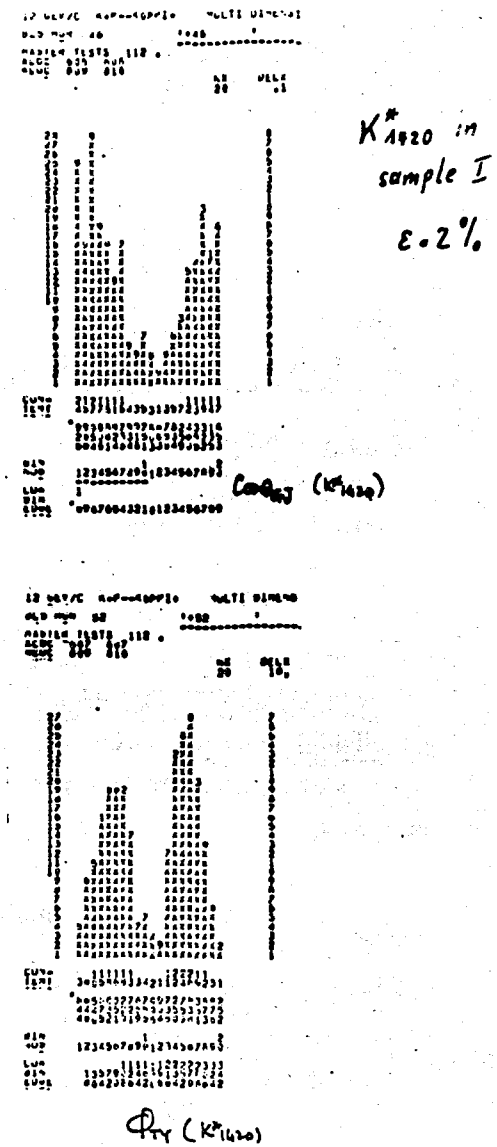

Fig. 18. Gottfried-Jackson decay angular distribution and Treiman-Yang angular distribution for K*(1420) with cut-off ϵ = 2%.

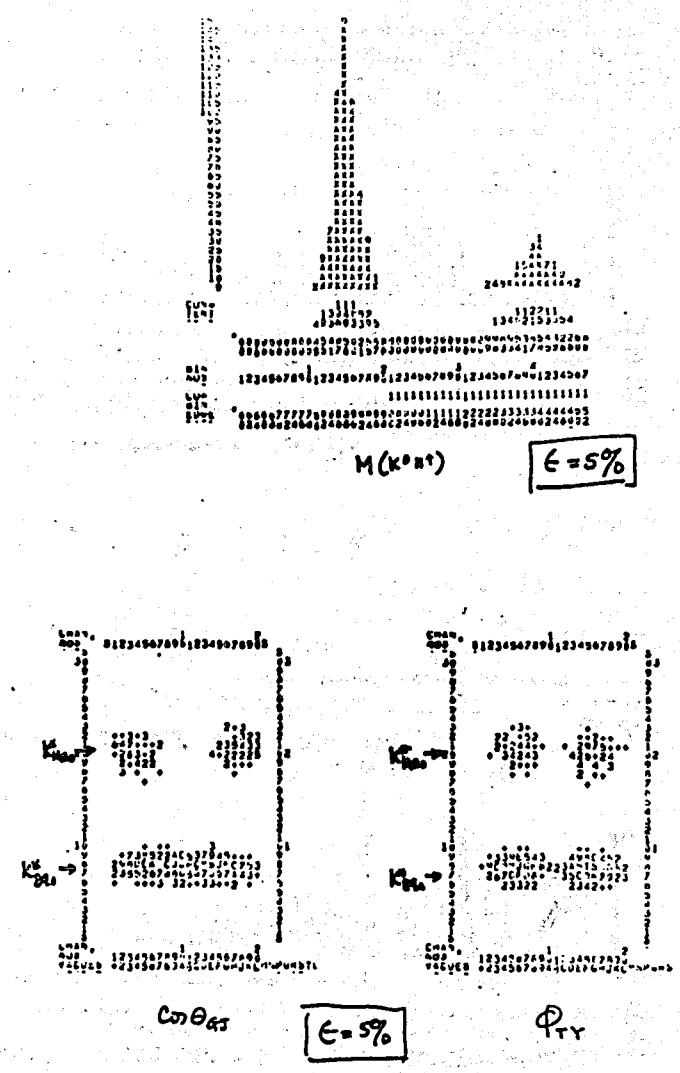

Fig. 19. Gottfried-Jackson decay angular distribution and Treiman-Yang angular distribution for K*(1420) with cut-off ϵ = 5%.

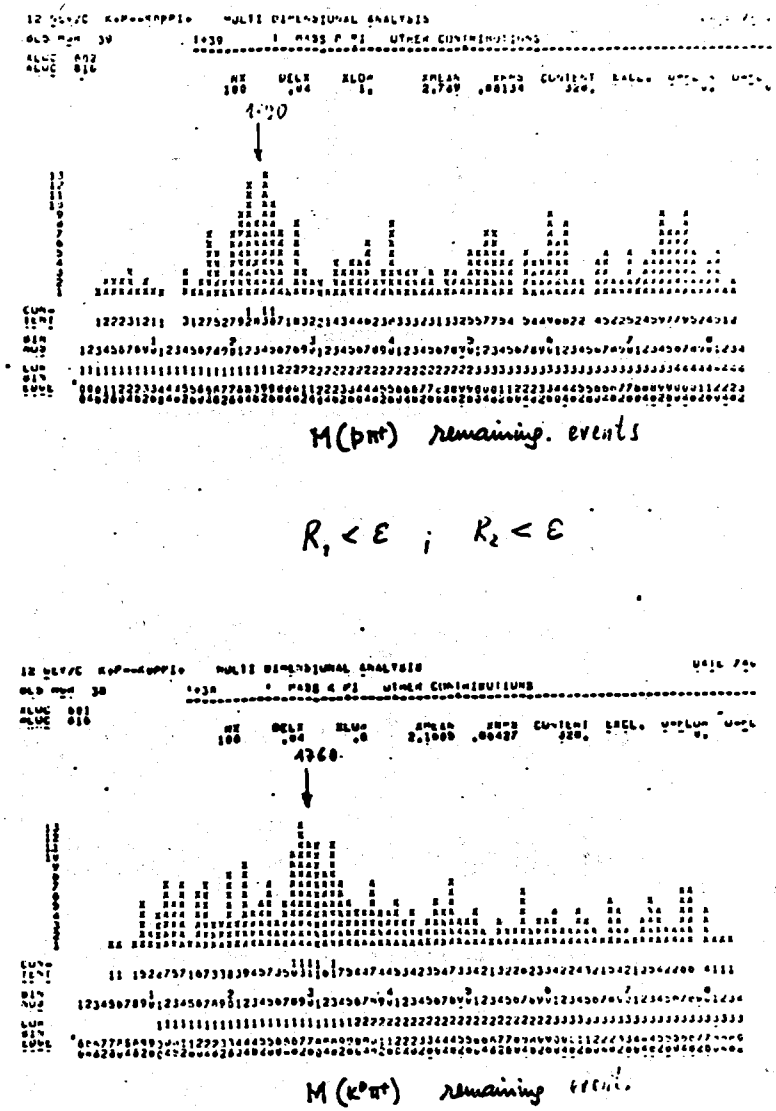

Fig. 20. Mass distributions $M(K^\circ\pi^+)$ and $M(p\pi^+)$ for remaining events with $R_1 < \epsilon$ and $R_2 < \epsilon$.

4.1. Resonance production and reaction mechanisms in 5- and 6-body final states

A quantitative investigation [21] of resonance production and reaction mechanisms for special subsamples was done at 16 GeV/c in the following reactions

$$\pi^+ p \rightarrow 3\pi^+ + 2\pi^- + p$$

$$\pi^- p \rightarrow 2\pi^+ + 3\pi^- + p$$

using simplified LPS techniques. The populations of the different LPS sectors are given in table 2a and 2b. Böttcher et al. get the following results:

(i) The cross sections (corrected for phase space) of the individual LPS configurations of the final state particles show the characteristic behaviour known for three- and four-body final states. Sectors which are dominated by diffractive processes have cross sections consistent with being energy independent (see column 8 of table 2).

(ii) Results are obtained consistent with the existence of diffractive dissociation (DD) of the incident pion into five pions and of the target proton into proton and four pions (see table 2 and fig. 21). The pion DD is 1.5 - 2 times stronger than the proton DD. The upper limits of the cross sections for these processes in π^+ and π^- induced reactions, respectively are similar, $\lesssim 42(38)\ \mu b$ for the pion DD; $\lesssim 22(25)\ \mu b$ for the proton DD in $\pi^+ p$ ($\pi^- p$).

(iii) It is shown that double diffractive dissociation is not a dominating reaction mechanism (see table 2 and fig. 22).

(iv) As you can see from fig. 23 the production of a backward going $\Delta(1950)$ was observed which decays mainly into $p\pi^+\pi^+\pi^-$ and much more weakly into $p\pi^+\pi^-\pi^-$.

Table 2a

POPULATION OF LPS SECTORS FOR $\pi^+ p \rightarrow p\,\pi^+\pi^+\pi^+\pi^-\pi^-$

sector	forward	backward	events (exp.)	percentage (exp.)	percentage (CPS)	R (exp./CPS)	n (energy-dep.)
P 1	+ + + − −	p	320 ± 18	11.0 ± 0.6	1.9 ± 0.2	5.8 ± 0.7	0.4 ± 0.4
P 2	+ + − −	p^+	716 ± 27	24.6 ± 0.9	11.0 ± 0.3	2.2 ± 0.1	0.8 ± 0.2
P 3	+ + + −	p^-	199 ± 14	6.8 ± 0.5	7.4 ± 0.3	0.9 ± 0.1	1.5 ± 0.4
P 4	+ − −	p^{++}	300 ± 17	10.3 ± 0.6	13.9 ± 0.4	0.7 ± 0.1	2.0 ± 0.3
P 5	+ + −	p^{+-}	648 ± 25	22.2 ± 0.9	27.8 ± 0.6	0.8 ± 0.1	1.4 ± 0.2
P 6	+ + +	p^{--}	36 ± 6	1.2 ± 0.2	4.6 ± 0.2	0.3 ± 0.1	1.2 ± 1.1
P 7	− −	p^{+++}	16 ± 4	0.5 ± 0.1	2.9 ± 0.2	0.2 ± 0.1	4.6 ± 1.1
P 8	+ −	p^{++-}	420 ± 21	14.4 ± 0.7	17.4 ± 0.4	0.8 ± 0.1	1.1 ± 0.3
P 9	+ +	p^{+--}	147 ± 12	5.0 ± 0.4	8.7 ± 0.3	0.6 ± 0.1	1.9 ± 0.5
P 10	−	p^{+++-}	12 ± 3	0.4 ± 0.1	1.8 ± 0.2	0.2 ± 0.1	0.1 ± 1.7
P 11	+	p^{++--}	102 ± 10	3.5 ± 0.3	2.6 ± 0.3	1.4 ± 0.1	0.3 ± 0.7
P 12	p, mesons	mesons	198 ± 14				3.5 ± 0.3

Table 2b

POPULATION OF LPS SECTORS FOR $\pi^- p \rightarrow p\,\pi^+\pi^+\pi^-\pi^-\pi^-$

sector	forward	backward	events (exp.)	percentage (exp.)	percentage (CPS)	R (exp./CPS)	n (energy-dep.)
M 1	+ + − − −	p	143 ± 12	12.3 ± 1.0	1.9 ± 0.2	6.5 ± 0.9	−0.2 ± 0.2
M 2	+ − − −	p^+	148 ± 12	12.7 ± 1.0	7.4 ± 0.3	1.7 ± 0.2	0.7 ± 0.2
M 3	+ + − −	p^-	175 ± 13	15.1 ± 1.1	11.0 ± 0.3	1.4 ± 0.1	1.0 ± 0.1
M 4	− − −	p^{++}	44 ± 7	3.8 ± 0.6	4.6 ± 0.2	0.8 ± 0.1	0.7 ± 0.3
M 5	+ − −	p^{+-}	267 ± 16	22.9 ± 1.4	27.8 ± 0.6	0.8 ± 0.1	0.6 ± 0.4
M 6	+ + −	p^{--}	67 ± 8	5.8 ± 0.7	13.9 ± 0.3	0.4 ± 0.1	1.2 ± 0.1
M 7	+ +	p^{---}	9 ± 3	0.8 ± 0.3	2.9 ± 0.2	0.3 ± 0.1	no events at 25 GeV/c
M 8	− −	p^{++-}	77 ± 9	6.6 ± 0.7	8.7 ± 0.3	0.8 ± 0.1	0.9 ± 0.3
M 9	+ −	p^{+--}	157 ± 13	13.5 ± 1.1	17.4 ± 0.4	0.8 ± 0.1	0.7 ± 0.2
M 10	+	p^{+---}	3 ± 2	0.3 ± 0.2	1.8 ± 0.2	0.2 ± 0.1	no events at 25 GeV/c
M 11	−	p^{++--}	72 ± 9	6.1 ± 0.7	2.6 ± 0.2	2.3 ± 0.3	−0.2 ± 0.3
M 12	p, mesons	mesons	63 ± 8				2.7 ± 0.3

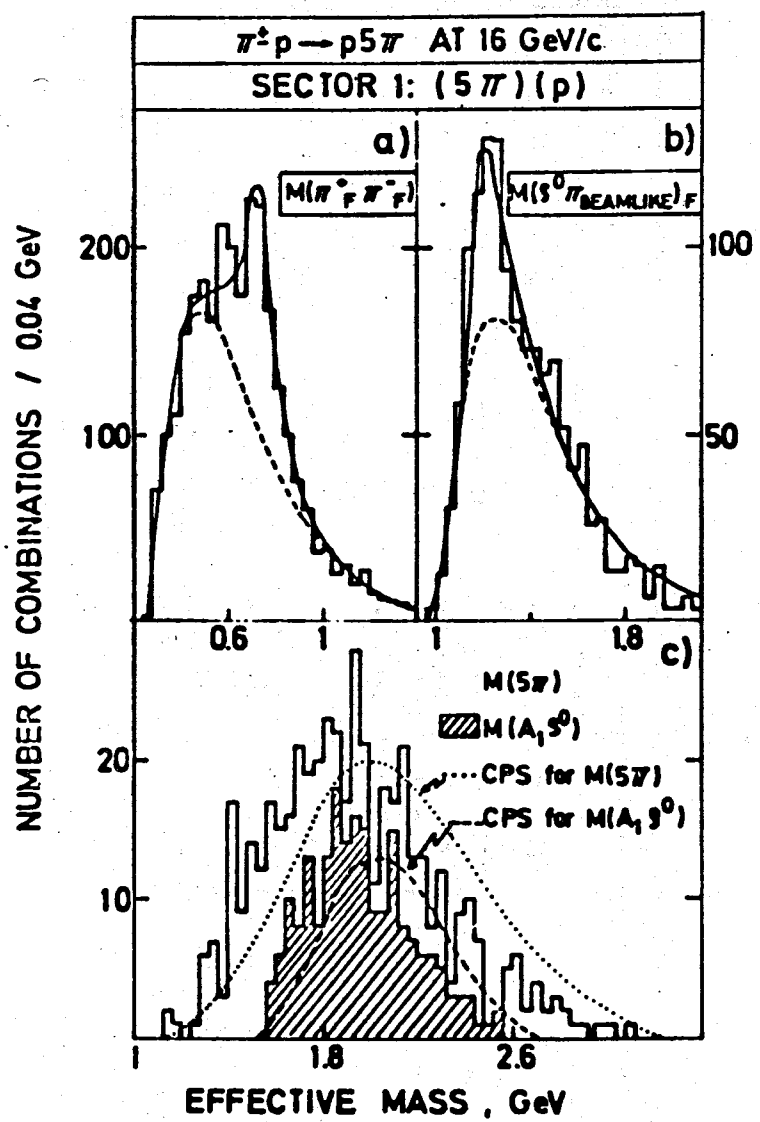

Fig. 21. Effective mass distribution for the $(\pi^+_F \pi^-_F)$, $(\rho^\circ \pi_{BEAML.})_F$ and $(5\pi)_F$ systems in sector 1. The results of the Breit-Wigner fit are given by full lines. Dashed and dotted lines represent CPS-background. In (c) the CPS curves are normalized to the experimental distributions,

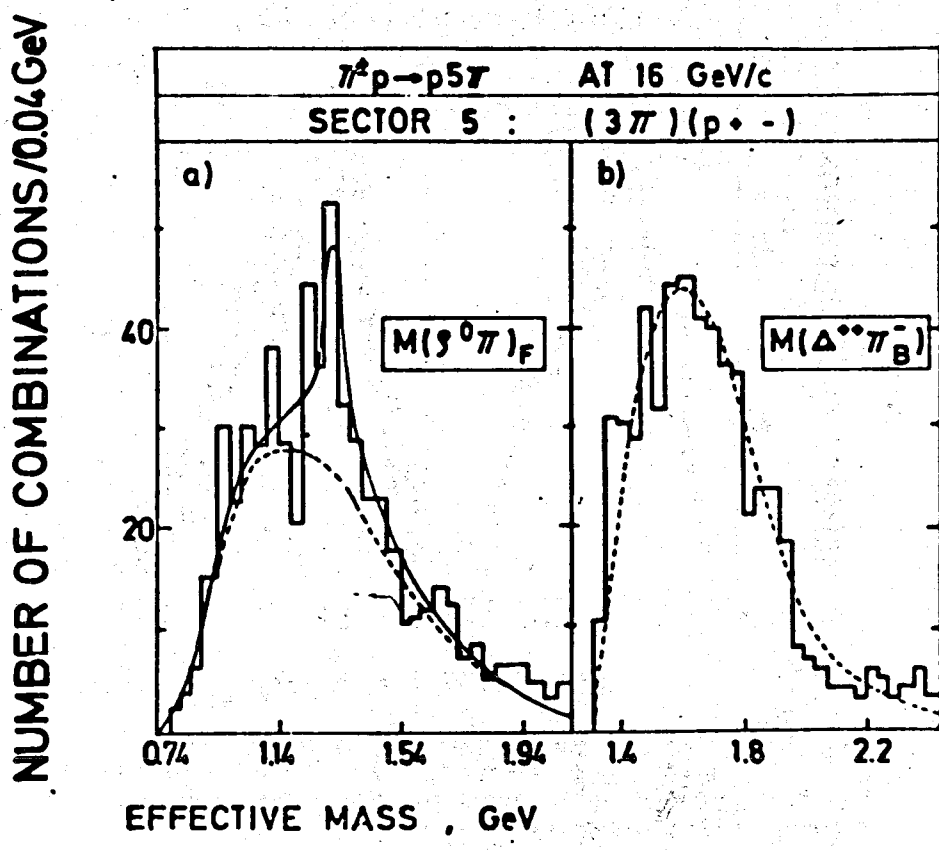

Fig. 22. Effective mass distribution for the $(\rho^\circ_F \pi_F)$ and $(\Delta^{++}_B \pi^-_B)$ system in sector 5. In a) the full line gives the result for a A_2 Breit-Wigner fit. In b) the CPS background is normalized to the experimental distribution.

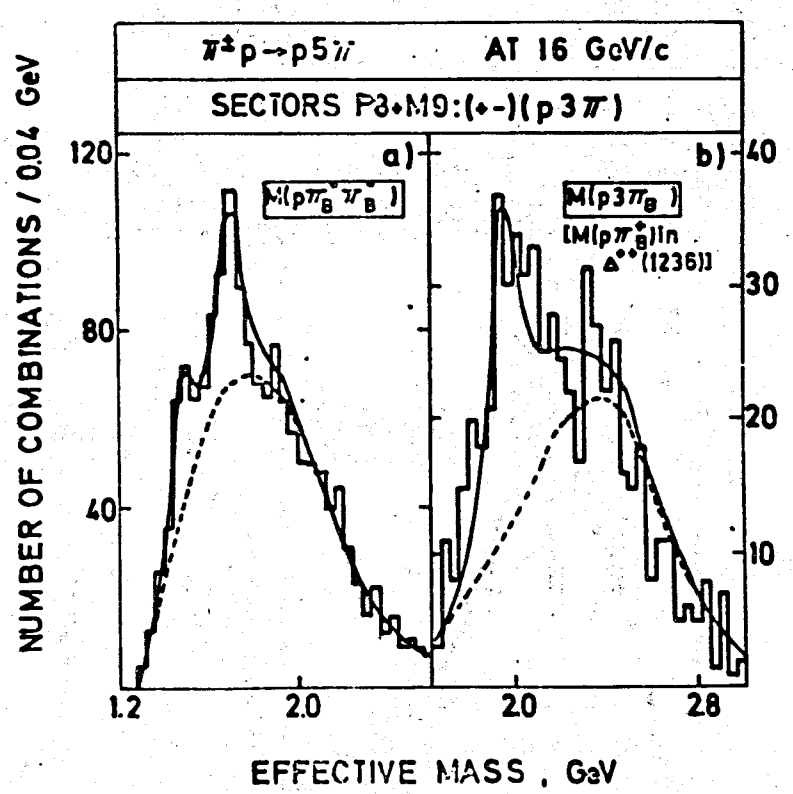

Fig. 23. Effective mass distribution for the $(p\pi_B^+\pi_B^-)$ and $(\Delta_B^{++}2\pi_B)$ systems in P8 + M9. The results of the Breit-Wigner fit are given by full lines. Dashed lines represent CPS background.

The quasi two body process $\pi^+p \to \Delta^{++}(1950)\rho^\circ$ occurs with a cross section of $(3.1 \pm 0.9)\,\mu b$.

(v) There is some indication for the quasi three body process $\pi^+p \to \rho^\circ\rho^\circ\Delta^{++}(1236)$ in sector P2,

(vi) Strong production of $\Delta^{++}(1236)$ in the backward hemisphere and $\rho^\circ(765)$, $f^\circ(1260)$ in the forward hemisphere are observed. ρ° is also emitted frequently in the backward direction (see fig. 24). $\Delta^\circ(1236)$, $N^*(1470)$, $N^*(1700)$, A_2 and possibly A_1 and $A_{1,5}$ are produced.

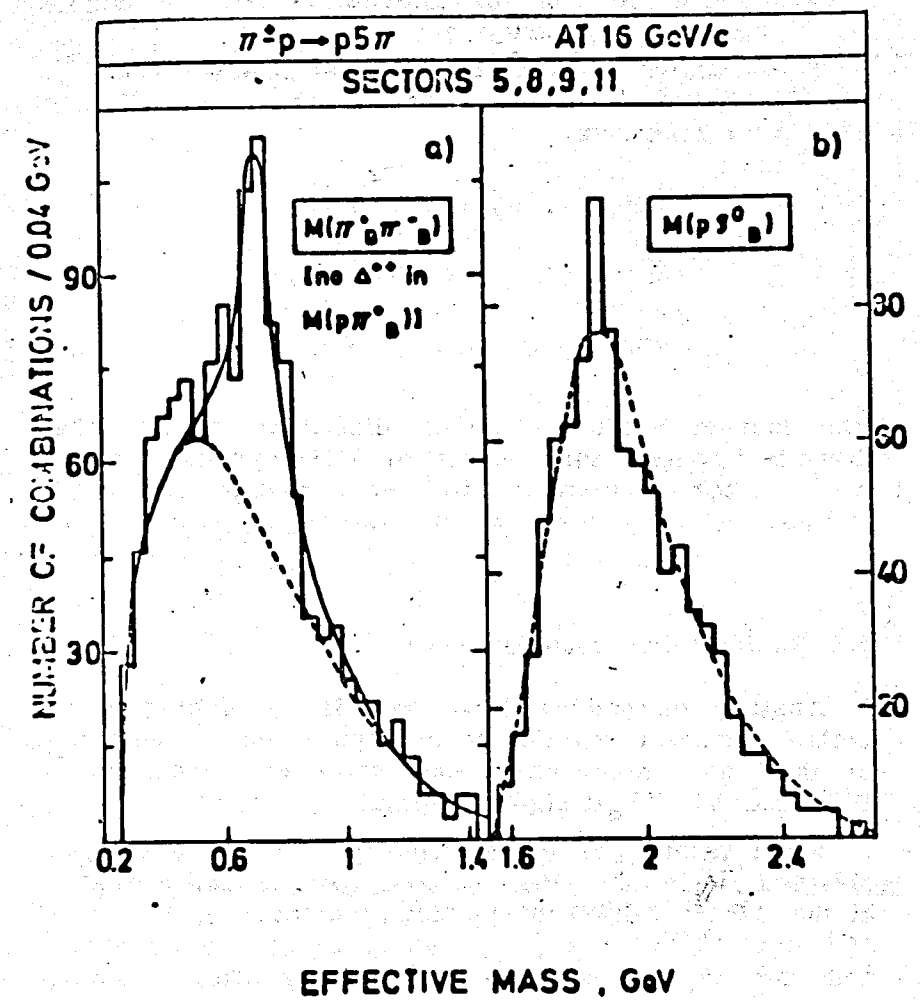

Fig. 24. Effective mass distribution for the $(\pi_B^+\pi_B^-)$ and $(p\rho_B^\circ)$ systems. The results of the Breit-Wigner fit are given by full lines. In b) the CPS background (dashed line) is normalized to the experimental distribution.

(vii) About 30% of the interactions go via double resonance production.

The Amsterdam - CERN - Nijmegen Collaboration /22/ has found the simultaneous production of $\Lambda(1520)$ and ω° in the reactions

$$K^- p \to (K^- p)(\pi^+ \pi^- \pi^\circ)$$

$$K^- p \to (\Sigma^\pm \pi^\mp)(\pi^+ \pi^- \pi^\circ)$$

$$K^- p \to (\Lambda \pi^+ \pi^-)(\pi^+ \pi^- \pi^\circ) .$$

The four-momentum transfer distributions show that there is a roughly equal amount of $\Lambda(1520)$ produced at the kaon vertex (nonstrange baryon exchange) as at the proton vertex (strange meson exchange) (see fig. 25).

4.2. Rapidity dispersion analysis

Another method of data analysis to identify if not isolate different reaction mechanisms, which contribute to the same many-body final state was proposed by Berger et al. /23/ at high energies.

First results of these rapidity dispersion analysis obtained from the Pisa - Stony Brook Collaboration at the ISR /24/ exhibit interesting structures in the $\delta^{(1)}$ vs. $\bar{\eta}^{(1)}$ plot. $\delta^{(1)}$ and $\bar{\eta}^{(1)}$ are the rapidity dispersion and the average rapidity respectively after rejecting the two charged particles with η_{max} and η_{min} respectively. The peaks with small (large) $\bar{\eta}^{(1)}$ and small $\delta^{(1)}$ were identified with target (beam) diffraction dissociation.

A similar analysis was made for $\pi^+ p \to (5\pi)^+ p$ at 16 GeV/c /21/. As expected, the structures observed are not as significant as at ISR energies (fig. 26a). However, you observe qualitatively the same properties. This is

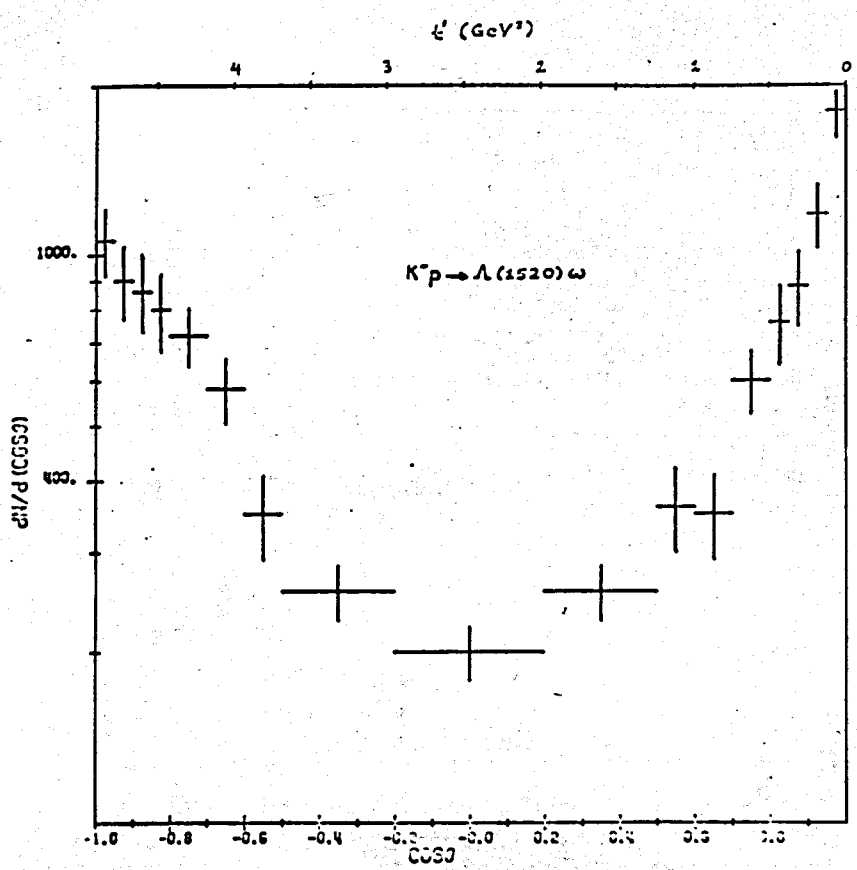

Fig. 25. Production angular distribution for the reaction

$$K^- p \to \Lambda(1520)\omega . \; (\cos\theta = \hat{p}_{\Lambda(1520)} \cdot \hat{p}_p) .$$

demonstrated in fig. 26b by the location of the diffractive events in the plot. In addition fig. 26c shows that events going to a large part via the reactions $\pi^+ p \to \Delta^{++}(1950)\rho^\circ$ and $\pi^+ p \to \Delta^{++}(1236)\rho^\circ\rho^\circ$ cover the production from the central region.

A rapidity dispersion analysis is being made on events of the exclusive reactions

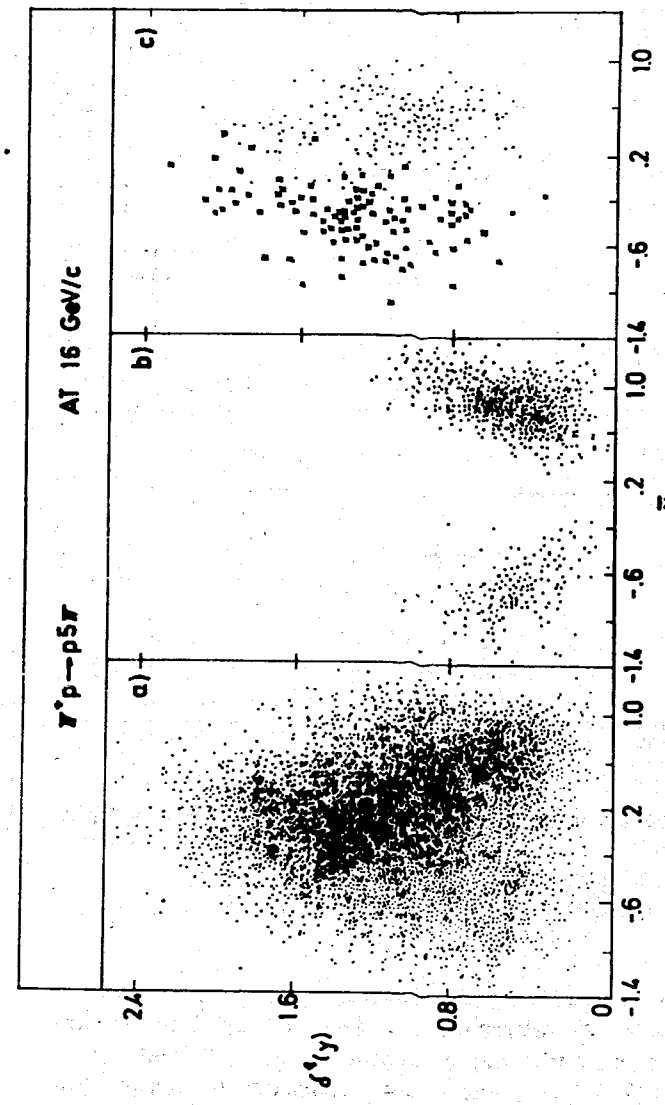

Fig. 26. $\pi^+ p \to p5\pi$ $\delta^{(1)}(y)$ vs. $\bar{y}^{(1)}$ a) all events. b) LPS sector P1 (right-hand). LPS sector P11 (left-hand). c) crosses LPS sector P8 , $1.8 < M(p\pi^+\pi_B^+\pi_B^-) < 2.12$ GeV ($\cong \Delta(1950)$) $M(\pi_F^+\pi_F^-)$ in ρ°. Points: LPS sector P2 $M(p\pi_B^+)$ in $\Delta^{++}(1236)$, M, $(\pi_{F1}^+\pi_{F1}^-)$ in ρ° $M(\pi_{F2}^+\pi_{F2}^-)$ in ρ°.

$\pi p \to 3\pi p$

$\pi p \to 5\pi p$

$\pi p \to 7\pi p$

at 8, 16 and 23 GeV/c [25]. Pion and baryon dissociation in the four particle channel are fairly clearly isolated by the dispersion technique at these energies. For high multiplicity reactions, it suffers (as do all inclusive techniques) by comparison with fully differential analyses. Nevertheless, the preliminary results of this analysis show that the technique should be a useful aid to pattern recognition and separation of dynamical mechanisms at NAL and ISR energies. This method should work even for data where one can measure, e.g., only angles of tracks, a situation where other methods of separation will probably fail.

4.3. Statistical analysis of clustering

An approach of clustering effects in many-particle final state was done by Ludlam and Slansky [26]. They define clustering in terms of the existence of two or more population centers in the full phase space. A nonclustering result is obtained if these points occupy a single, simply connected region of phase space.

This statistical analysis of clustering involves studying the fluctuations of the distribution of rapidities of each event about the average distribution.

Consider a date sample of N events, where n rapidities (or other kinematic variables) are measured in each event. The distribution density of $n \cdot N$ rapidities is denoted by $p(y)$, and the cumulative distribution function is defined by

$$F(y) = \int_{-\infty}^{y} dy' p(y')$$

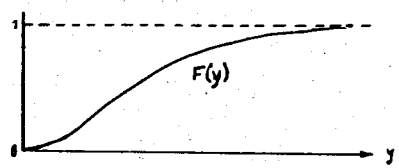

Each event is represented by a step function $S_n(y)$ of n steps of height $1/n$ at each of the rapidities.

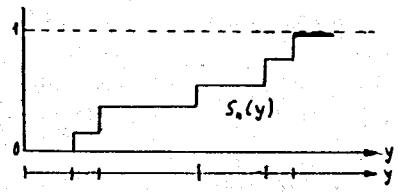

The fluctuation measure to investigate the clustering of secondaries is

$$M(y) = p(y) \cdot \langle [S_n(y) - F(y)]^2 \rangle$$

or

$$\langle \omega_n^2 \rangle = \int_{-\infty}^{\infty} M(y)\, dy$$

The experimental values of $M(y)$ and/or $\langle \omega_n^2 \rangle$ are to be compared with reference models. These models must belong to single mechanism processes (e.g., CPS) which give no clustering by definition.

The analysis was applied to 13 GeV/c $K^- p$ data[27] to the reaction $pp \to p p \pi^+ \pi^+ \pi^- \pi^-$ at 19 GeV/c[28], and to NAL data obtained from 205 GeV/c and 303 GeV/c proton-proton collisions[29] with the following results:

(i) The known differences in the clustering behaviour of the reactions $K^- p \to K^- \pi^+ \pi^- p$ and $K^- p \to \bar{K}^0 \pi^- \pi^0 p$ are readily distinguished.

(ii) Strong clustering is present in the reaction $K^- p \to K^- \pi^+ \pi^- \pi^0 p$.

(iii) Clustering is present in the reaction $p p \to p p \pi^+ \pi^+ \pi^- \pi^-$ which is mainly caused by events with one of the secondary protons clearly separated in rapidity from the other final state particles.

(iv) The results of the analysis at 205 GeV/c and 303 GeV/c proton-proton collisions suggest that even events of high multiplicity show clustering effects.

(v) The average cluster size appears to be independent of the multiplicity of the final state.

(vi) The nature and the extent of this structure need further investigation.

4.4. Multidimensional study of clustering

Under the assumption that two or more population centers exist in the full phase space a multidimensional study of clustering was done in the reaction $\pi^+ p \to p \pi^+ \pi^+ \pi^-$ at 8 GeV/c by Böttcher et al.[30] in order to test their method.

To find these clusters the authors used a method suggested by Koontz and Fukunaga[31]. This method does not need a priori knowledge about the clusters and uses for the classification of one event the kinematical information from the whole sample.

The aim of any cluster analysis is the assignment of space points to classes according to some criteria, e.g., the closeness of the points. The above mentioned cluster algorithm is derived from the criterion which minimizes the information loss due to the replacement of vector X_r (vector X_r being the kinematical variables defining the r-th event) by a set of labels ω_r (cluster

number). A special solution of this problem is obtained by the application of the following procedure:

(i) Choose randomly an initial classification of events.

(ii) For each vector X_r count the numbers of vectors within a suitable chosen distance R of X_r that are assigned to each class.

(iii) Reclassify each X_r to the class with the largest number of members within the distance R of X_r.

(iv) If any vector is placed in a new class repeat from step (ii). Otherwise stop.

By this procedure the boundary separating two classes moves away from the higher concentration towards valleys in the density distribution of the phase space. Figure 27 illustrates the action of this procedure on a two dimensional data set.

The method was applied to 4400 four-prong events. The following table gives the population of the clusters.

cluster	1	2	3	4	5	6	7	8	9	10
events	1355	879	651	188	246	232	255	330	76	168

These clusters, found by a purely statistical method, have correspondence to dynamical mechanisms. This is illustrated by the following distributions. For cluster 1 in fig. 28 a clear Δ^{++} and ρ_f^0 respectively is seen. Neither the $(p\pi_s^+\pi^-)$ nor the $(\pi_f^+\pi^+\pi^-)$ mass distribution show any resonance structure. Therefore in cluster 1 most of the events proceed via the channel $\pi^+ p \to \rho^0 \Delta^{++}$.

For cluster 5 in fig. 29 a clear signal in the A_1 mass region is seen. This (3π) system decays mainly via $(\rho_f^0\ \pi)$. The $t(p/p)$ distribution supports the interpretation of this cluster being A_1 production.

The analysis shows that there are still clusters to which more than one channel contribute. This overlapping could be due to the relatively low energy. Therefore it seems worthwhile to apply this method at higher energies.

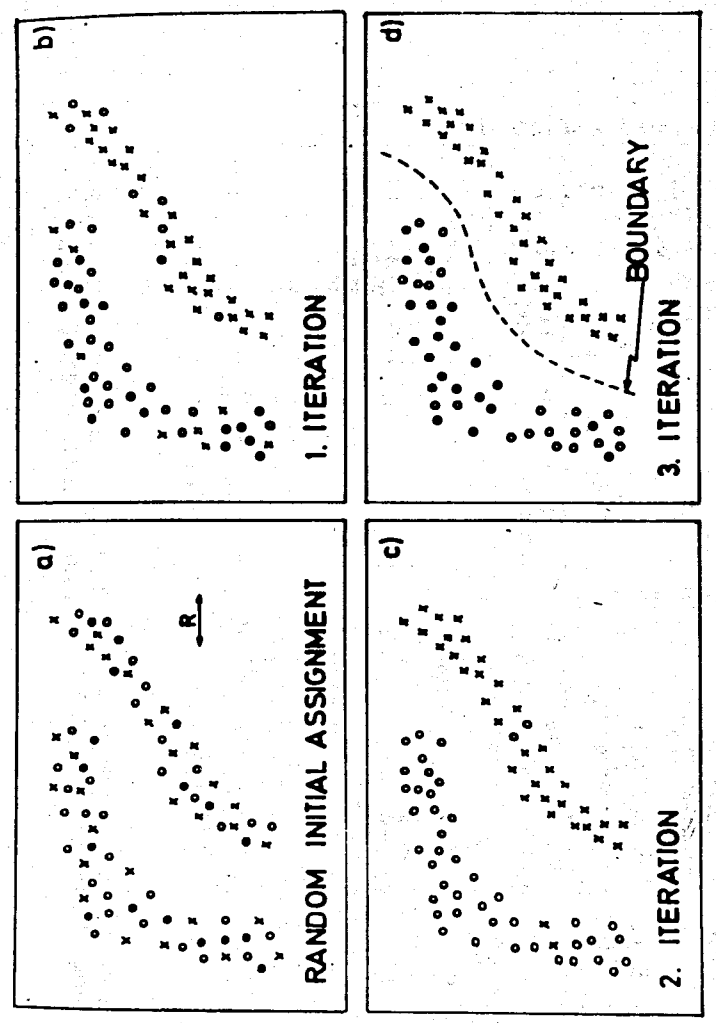

Fig. 27. Working scheme of the Valley-Seeking Technique to find clusters illustrated at a two-dimensional data set. The choice of R is indicated by the arrow. a) Random initial assignment of the points into three classes o, x and •. b) Reassignment of the points after the 1st iteration. c) Reassignment of the points after the 2nd iteration. d) Final assignment of the points into two classes. One class has become empty during the iterations.

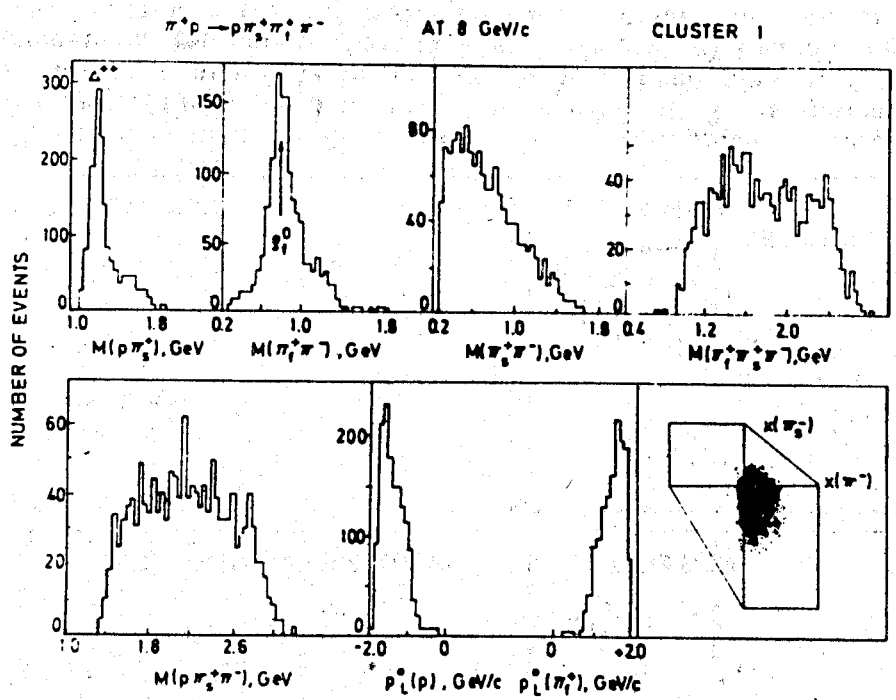

Fig. 28. Effective mass distributions, longitudinal momentum distributions and LPS plot characterizing cluster 1.

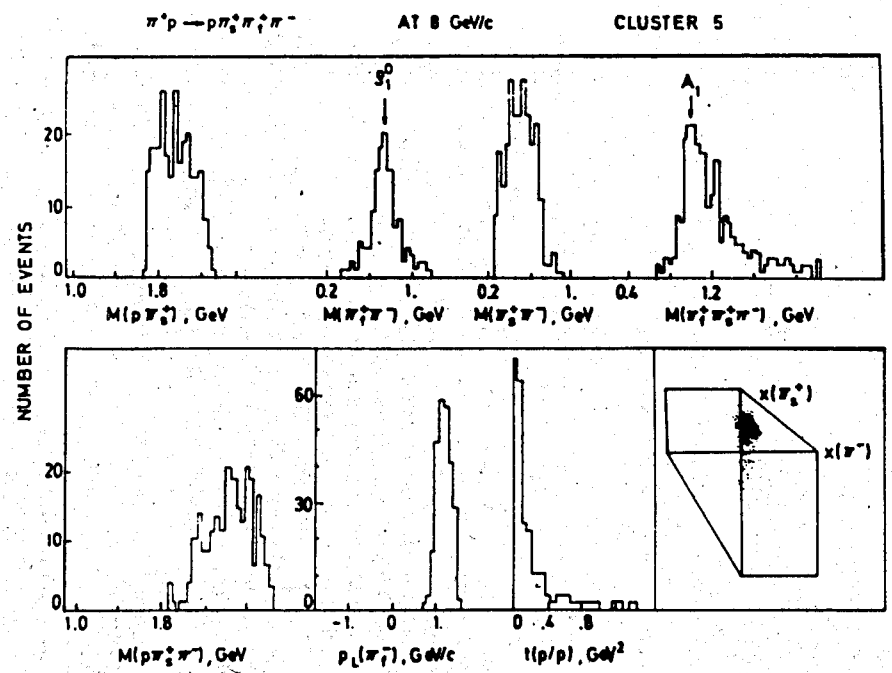

Fig. 29. Effective mass distributions, longitudinal momentum distribution of the π_f^+, the four momentum transfer between the incoming and outgoing proton, and the LPS plot characterizing cluster 5.

The application of new methods which allow a differential analysis of exclusive reactions has already lead to a better understanding of the reaction mechanism. We may expect that the further study with these methods, will help to understand the less differential results obtained at NAL and ISR energies.

References

1. G.Ascoli et al. Phys.Rev.Lett., 25, 962 (1970); Phys.Rev.Lett., 26, 929 (1971); Phys.Rev., D7, 669 (1973).
2. CERN - Serpukhov Collaboration, Yu.M.Antipov et al. Nucl.Phys., B63, 153 (1973).
3. G.Thompson et al. Phys.Rev.Lett., 32, 331 (1974); Nucl. Phys., B69, 381 (1974).
4. Aachen - Berlin - Bonn - CERN - Heidelberg Collaboration, "Partial wave analysis of the 3π system produced in the reaction $\pi^+p \to (\pi^+\pi^+\pi^-)p$ at 8, 16 and 23 GeV/c", to be submitted to Nucl.Phys.,B.
5. G.Ascoli et al. "The $A_2 - A_1$ interference phase", COO - 1195 - 285, ILL - (TH) - 74 - 5, April, 1974.
6. Aachen - Berlin - CERN - London - Vienna Collaboration, M.Deutschmann et al. CERN/D.Ph.II/Phys., 74-1, to be submitted to Phys.Lett. B.
7. Rutherford - Ecole Polytechnique - Saclay Collaboration, "A study of the Q enhancement in the reaction $K^-p \to K^-\pi^-\pi^+p$ at 14.3 GeV/c", submitted to the 5th International Symposium on Many Particle Hadrodynamics, June,1974, Eisenach - Leipzig.
8. CERN - Serpukhov Collaboration, submitted to the 4th International Conference on Experimental Meson Spectroscopy, April, 1974.
9. Aachen - Berlin - CERN - London - Vienna and Athens Democritus - Liverpool - Vienna Collaboration. "The spin-parity structure of the $(K^-\pi^+)$ and $(\bar{K}^0\pi^+\pi^-)$ systems produced in charge exchange", CERN/D.Ph.II/ DIVERS 74-2, presented at the IX Recontre de Moriond, March 1974.
10. Aachen - Berlin - CERN - London - Vienna Collaboration, "Spin parity structure of the $(K\pi)$ system produced in the reaction $K^-p \to (K^-\pi^+)n$"(unpublished).
11. D.Cords et al. Nucl.Phys., B54, 109 (1973).

12. H.H.Bingham et al. Nucl.Phys., B41, 1 (1972). R.Mercer et al. Nucl.Phys., B32, 381 (1971). H.Yuta et al. Phys.Rev.Lett., 26, 1502 (1971). A.Firestone et al. Phys.Rev.Lett., 26, 1460 (1971). C.Y.Chien et al. Phys.Lett., B28, 143 (1968).
13. J.E.Brau et al. Phys.Rev.Lett., 27, 1481 (1971).
14. L. Van Hove. "A modified prism plot analysis", presented to the Topical Conference on Multidimensional Analysis of Hadron Collisions, February, 1974, CERN; "Multidimensional analysis and parametric fitting of few body collisions data", Proceedings of the IVth International Symposium on Multiparticle Hadrodynamics, edited by F.Dumio, A.Giovanni, S.Ratti; Pavia, 1973, p. 439.
15. D.B.Bastien et al. "Diffractive processes in $\bar{p}p$ interactions at 5.1 GeV/c", submitted to the Vth Internat. Symposium on Many Particle Hadrodynamics, June, 1974, Eisenach - Leipzig.
16. Ferrando et al. CERN/D.Ph.II/Phys., 73-49.
17. P.J.Dornan and B.Pollock. "A variant of the PPA method", presented to the Topical Conference on Multidimensional Analysis of Hadron Collisions, February, 1974, CERN .
18. A.Ferrando. "A modified prism plot analysis applied to $K^+p \to pK^0\pi^+$ at 5 GeV/c", presented to the Topical Conference on Multidimensional Analysis of Hadron Collisions, February, 1974, CERN.
19. N.Yamdagni. "Analytical Multichannel Analysis of the Reaction $K^+p \to pK^0\pi^+$ at 12 GeV/c", presented to the Topical Conference on Multidimensional Analysis of Hadron Collisions, February, 1974, CERN.
20. N.Yamdagni. "Prism plot analysis of $K^+p \to K^0\pi^+p$ at 5 and 12 GeV/c". Proceedings of the IVth International Symposium on Multiparticle Hadrodynamics, edited by F.Dumio, A.Giovanni, S.Ratti; Pavia, 1973, p. 388.
21. H.Böttcher et al. "Study of the six body final states on $\pi^\pm p$ interactions at 16 GeV/c", Berlin, PHE 74-2, submitted to the Vth International Symposium on Many Particle Hadrodynamics, June, 1974, Eisenach - Leipzig.
22. Amsterdam - CERN - Nijmegen Collaboration. "The production of $\Lambda(1520)\omega$ in 5- and 6-body K^-p final states at 4.2 GeV/c", submitted to the Vth International Symposium on Many Particle Hadrodynamics, June,1974, Eisenach - Leipzig.
23. E.L.Berger et al. Phys.Lett., 43B, 132 (1973).
24. CERN - Pisa - Stony Brook Collaboration, L.Foa,

IInd Aix-en-Provence Conference on Elementary Particles, Journal de Physique 34, C1 (1973).
25. Aachen - Berlin - Bonn - CERN - Cracow - Heidelberg - Warsaw Collaboration. U.Gensch, private communication.
26. T.Ludlam and R.Slansky. Phys.Rev., D8, 1408 (1973).
27. J.Hanlon et al. Phys.Lett., 46B, 415 (1973).
28. J.Allan et al. "Investigation of possible clustering effects in the reaction $pp \to p\,p\,\pi^+\pi^+\pi^-\pi^-$ at 19 GeV/c", submitted to the Vth International Symposium on Many Particle Hadrodynamics, June, 1974, Eisenach - Leipzig.
29. T.Ludlam et al. Phys.Lett., 48B, 449 (1974).
30. H.Böttcher et al. "A multidimensional study of clustering in the reaction $\pi^+ p \to p\,\pi^+\pi^+\pi^-$ at 8GeV/c". Berlin, PHE 74-1, submitted to the Vth International Symposium on Many Particle Hadrodynamics, June, 1974, Eisenach - Leipzig.
31. W.L.Koontz and K.Fukunaga. IEEE Transactions on computers, C-21, 2 (72).

Received by Publishing Department
on June 28, 1974.